LETTER

https://doi.org/10.1038/s41586-018-0785-8

A male-expressed rice embryogenic trigger redirected for asexual propagation through seeds

Imtiyaz Khanday[1,2], Debra Skinner[1], Bing Yang[3], Raphael Mercier[4] & Venkatesan Sundaresan[1,2,5]*

The molecular pathways that trigger the initiation of embryogenesis after fertilization in flowering plants, and prevent its occurrence without fertilization, are not well understood[1]. Here we show in rice (*Oryza sativa*) that BABY BOOM1 (BBM1), a member of the AP2 family[2] of transcription factors that is expressed in sperm cells, has a key role in this process. Ectopic expression of *BBM1* in the egg cell is sufficient for parthenogenesis, which indicates that a single wild-type gene can bypass the fertilization checkpoint in the female gamete. Zygotic expression of *BBM1* is initially specific to the male allele but is subsequently biparental, and this is consistent with its observed auto-activation. Triple knockout of the genes *BBM1*, *BBM2* and *BBM3* causes embryo arrest and abortion, which are fully rescued by male-transmitted *BBM1*. These findings suggest that the requirement for fertilization in embryogenesis is mediated by male-genome transmission of pluripotency factors. When genome editing to substitute mitosis for meiosis (*MiMe*)[3,4] is combined with the expression of *BBM1* in the egg cell, clonal progeny can be obtained that retain genome-wide parental heterozygosity. The synthetic asexual-propagation trait is heritable through multiple generations of clones. Hybrid crops provide increased yields that cannot be maintained by their progeny owing to genetic segregation. This work establishes the feasibility of asexual reproduction in crops, and could enable the maintenance of hybrids clonally through seed propagation[5,6].

Understanding the molecular pathway that underlies the initiation of embryogenesis by a fertilized egg cell is a major unresolved problem in plant development[1]. In animals, the initiation of embryogenesis depends upon defined maternal factors[7]. In plants, two contrasting models have been proposed: one suggests that the two parental genomes contribute equally[8], whereas the other considers that the maternal genome has the primary role in early embryogenesis[9,10]. The identity and parental origin of the specific factors in plants that trigger zygotic development are as yet undetermined. We have previously used rice to elucidate transcriptome dynamics during the zygotic transition[11] and found that *BABY BOOM* (*BBM*)-like transcription factors of the APETALA 2/ETHYLENE RESPONSE FACTOR (AP2/ERF) superfamily[12] are expressed in zygotes after fertilization, which suggests a potential role in the initiation of embryogenesis (Extended Data Table 1a). *BBM* genes from *Arabidopsis thaliana* and *Brassica napus* can ectopically induce somatic embryos[13]; however, a role for these genes in the initiation of zygotic embryos has not been established[2]. We first determined that ectopic expression of *BBM1*—a *BBM*-like gene expressed in rice zygotes—also resulted in somatic embryos, both by examining their morphology and by using embryo marker genes (Extended Data Fig. 1a–d). Because *BBM1* expression increases with the age of the zygote[11] (Extended Data Table 1a), we investigated whether its expression is autoregulated, by inducing a constitutive BBM1–glucocorticoid receptor (GR) fusion in somatic tissues using dexamethasone (DEX) (Extended Data Fig. 1e). Quantitative PCR after reverse transcription (RT–qPCR), using allele-specific primers, showed that the expression of endogenous *BBM1*—but not the *BBM1-GR* fusion transgene—was highly induced after 24 h of DEX treatment (Extended Data Fig. 1f–h). This expression was maintained in the presence of the protein-biosynthesis inhibitor cycloheximide (CYC), indicating that BBM1 auto-activation is likely to be direct (Extended Data Fig. 1h). Auto-activation might be a conserved feature of *BBM* genes, because *B. napus* BABY BOOM can activate the expression of *Arabidopsis BBM*[14].

Our previous study of hybrid zygote transcriptomes[11] indicated that, although most zygotic transcripts were from the female genome, a few de novo transcription factors—including *BBM1*—had male-derived transcripts. We used RT–PCR amplification across single nucleotide polymorphisms (SNPs) in *BBM1* to confirm that, at 2.5 h after pollination (HAP) (corresponding to karyogamy), only the male *BBM1* allele is expressed in reciprocal crosses of *indica* and *japonica* cultivars[11] (Extended Data Fig. 2a). These results were confirmed in isogenic zygotes in the *japonica* Kitaake cultivar. We reciprocally crossed wild-type plants to transgenic plants that carried a translational fusion of the *BBM1* genomic locus to GFP (*BBM1-GFP*) (Extended Data Fig. 2b). Zygotes at 2.5 HAP displayed GFP expression only if the *BBM1-GFP* transgene was transmitted from the male parent (Fig. 1a). Consistent with this observation, in *BBM1-GFP* selfed progeny, GFP was detected in only about half of the zygotes, instead of the three-quarters ratio that would be expected if there is no parent-of-origin bias (Fig. 1a). Subsequently, GFP expression can be detected from the female allele in 6.5 HAP zygotes, corresponding to mid-to-late G2 phase (Extended Data Fig. 2c, d). Because BBM1 is capable of auto-activation of its own promoter (Extended Data Fig. 1h), the late expression of *BBM1* from the female allele might result from earlier expression of *BBM1* from the male allele. Other redundantly acting *BBM* genes might also contribute to this delayed activation (see below). *BBM1* expression continues through the later stages of embryo development (Extended Data Fig. 2e). In gametes, *BBM1* RNA can be detected by RT–PCR in sperm cells but not in egg cells (Extended Data Fig. 2f), which is consistent with RNA sequencing data[15] (Extended Data Table 1a). Furthermore, the BBM1–GFP fusion protein was expressed in sperm cells, which suggests that both transcription and translation of *BBM1* can occur in male gametes before fertilization (Extended Data Fig. 2g).

The expression of *BBM1* specifically from the male genome after fertilization, together with its capability to induce somatic embryogenesis, suggested that BBM1 could be a trigger of embryo development in the zygote (Extended Data Fig. 3a). In naturally apomictic (asexually reproducing) *Pennisetum squamulatum*, an apospory-specific locus contains multiple copies of a *BABY BOOM*-like gene that is expressed in egg cells before fertilization and induces parthenogenesis[16,17]. However, it is not known whether the BBM protein from the apomict has evolved novel capability in functional domains and interactions with other factors[16,17], or whether parthenogenesis might simply be a consequence of the expression pattern. To test whether wild-type rice BBM1 could initiate embryo development without fertilization, we ectopically expressed *BBM1* under an *Arabidopsis* egg-cell-specific promoter (*pDD45*)[18] that has previously been shown to confer egg-cell expression in rice[19] (Extended Data Fig. 3b, c). In emasculated flowers,

[1]Department of Plant Biology, University of California, Davis, CA, USA. [2]Innovative Genomics Institute, Berkeley, CA, USA. [3]Department of Genetics, Development and Cell Biology, Iowa State University, Ames, IA, USA. [4]Institut Jean-Pierre Bourgin, INRA, AgroParisTech, CNRS, Université Paris-Saclay, Versailles, France. [5]Department of Plant Sciences, University of California, Davis, CA, USA. *e-mail: sundar@ucdavis.edu

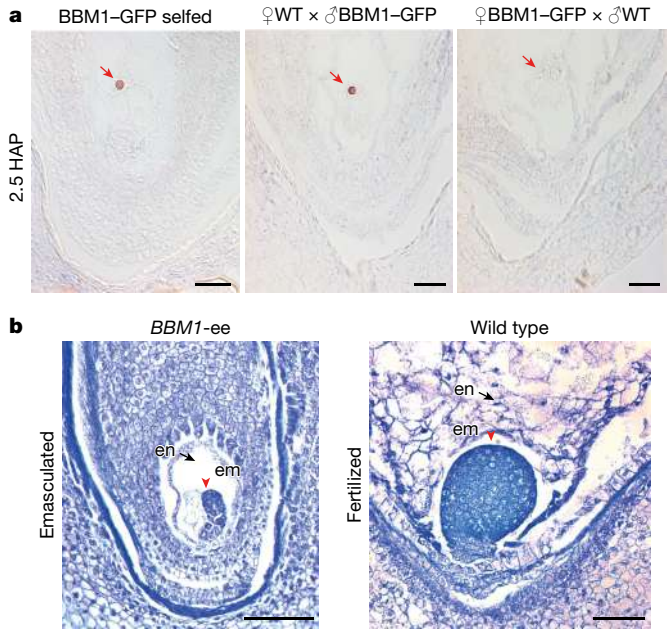

Fig. 1 | Paternal expression of *BBM1* in zygotes. a, Paternal allele-specific expression of *BBM1* in isogenic zygotes at 2.5 HAP. Expression of BBM1 fused to a GFP reporter was detected by antibody staining. GFP expression is observed only when BBM1–GFP is transmitted by the male parent ($n = 20$ for each panel, χ^2 test $P = 0.039$). Left, $n = 11/20$; middle, $n = 9/20$; right, $n = 0/20$. Red arrows point to zygote nuclei. WT, wild type. Scale bars, 25 μm. **b**, Development of parthenogenetic embryos (red arrowhead) by egg-cell-specific expression of *BBM1* in carpels of an emasculated *BBM1*-ee plant at nine days after emasculation ($n = 12/98$). In the absence of fertilization, endosperm development is not observed (black arrow). In fertilized control wild-type (4 days after pollination (DAP)) carpels, the development of both embryo (em; red arrowhead) and endosperm (en; black arrow) is observed ($n = 30$). Scale bars, 100 μm.

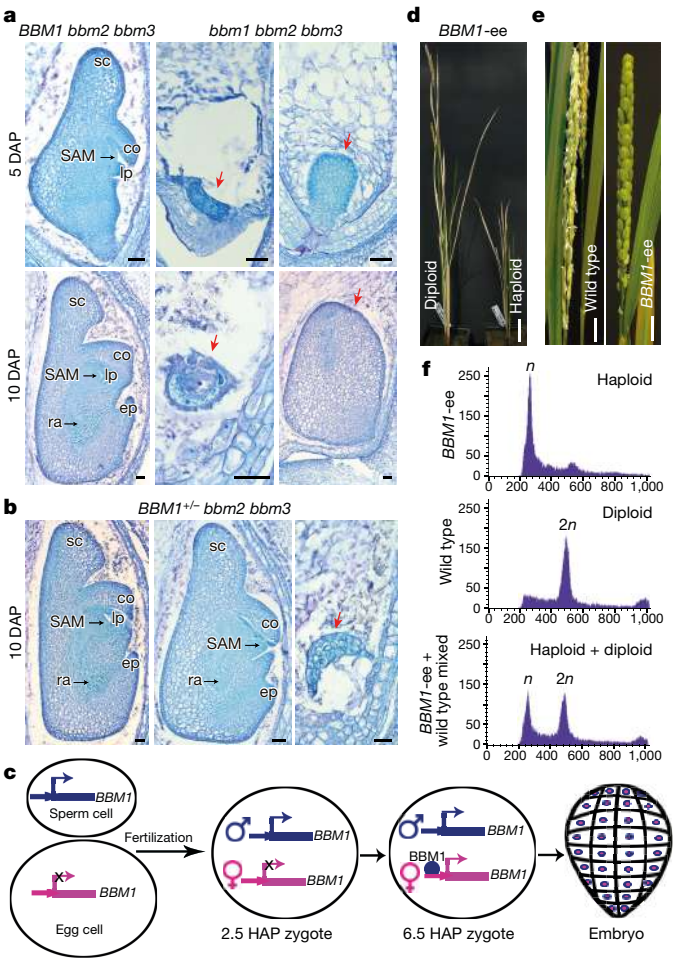

Fig. 2 | Phenotypes of *bbm1 bbm2 bbm3* mutant embryos and haploid induction. a, Embryos at 5 DAP (top) and 10 DAP (bottom). Embryos develop normally with wild-type *BBM1* ($n = 50$; left) but show an early arrest ($n = 24/82$; middle) or undergo a number of divisions without organ formation ($n = 58/82$; right) in *bbm1 bbm2 bbm3* triple homozygous mutant embryos. **b**, 10 DAP embryos that are heterozygous for *BBM1* but homozygous mutants for *bbm2* and *bbm3*. They show normal development ($n = 38/53$, left), are delayed ($n = 8/53$; middle), or show early arrest ($n = 4/53$; right). Scale bars, 100 μm. co, coleoptile; ep, epiblast; lp, leaf primordia; ra, radicle; SAM, shoot apical meristem; sc, scutellum. **c**, Schematic model of *BBM1* function in rice embryogenesis. **d**–**f**, Characterization of *BBM1*-ee induced haploids. **d**, Difference in height between parthenogenetic haploid and sexual diploid siblings ($n = 555$). Scale bar, 5 cm. **e**, A *BBM1*-ee parthenogenetic haploid panicle showing no anthesis (right) compared to an anthesis stage control wild-type panicle (left) ($n = 113$). **f**, Flow-cytometric DNA histograms for ploidy determination. Parthenogenetic haploid showing a 1*n* peak ($n = 19$, top), wild-type diploid with a 2*n* peak (middle) and a mixed sample of *BBM1*-ee and wild type showing 1*n* and 2*n* peaks (bottom).

we observed embryonic structures without endosperm development (Fig. 1b) in around 12% ($n = 98$) of ovules of *pDD45::BBM1* transformants (hereafter referred to as *BBM1*-ee, to denote *BBM1*-egg-cell expressed); these structures were absent in wild-type ovules ($n = 109$). Thus, the expression of a single wild-type transcription factor, BBM1, can overcome the requirement of fertilization for embryo initiation by an egg cell. The observation that a wild-type gene from a sexually reproducing plant is sufficient to induce parthenogenesis when misexpressed suggests that asexual reproduction could potentially evolve from the altered expression of existing genes within the sexual pathway.

Loss-of-function mutants of *BBM*-like genes in *Arabidopsis* and related plants have no embryonic phenotypes; consequently, their functions in early embryogenesis are as yet undefined[2]. Of the multiple *BBM*-like genes in rice, at least three—*BBM1*, *BBM2* and *BBM3* (Os11g19060, Os02g40070 and Os01g67410, respectively)—are consistently expressed in early zygotes (Extended Data Table 1a). We used the CRISPR–Cas9 system to generate *bbm1 bbm3* and *bbm2 bbm3* double mutants (Extended Data Fig. 4a, b), both of which were fully fertile. Crossing the double mutants and selfing (Extended Data Fig. 4c; see Methods) yielded no *bbm1 bbm2 bbm3* triple homozygous plants ($n = 52$). However, *BBM1/bbm1 bbm2/bbm2 bbm3/bbm3* plants were recovered and selfed (Extended Data Fig. 4d). Analysis of the progeny showed that approximately 36% failed to germinate (Extended Data Table 1b). Genotyping of the germinated seedlings suggested that the viability of the *bbm1 bbm2 bbm3* triple-mutant seeds was severely affected (2 out of 191 viable compared with the expected 48 out of 191; Extended Data Table 1b). *BBM1/bbm1 bbm2/bbm2 bbm3/bbm3* seedlings were also under-represented, which suggests that the viability of this genotype is also compromised (Extended Data Table 1b). A subset of the non-germinating seeds could be genotyped using their endosperm, and were found to be either homozygous or heterozygous for *bbm1* but not homozygous for *BBM1* (Extended Data Fig. 4e). The two *bbm1 bbm2 bbm3* triple homozygotes showed normal growth with no obvious vegetative or floral defects and produced normal seed sets, indicating that the *BBM1–BBM3* genes are not required for post-embryonic development. However, their progeny seeds failed to germinate (Extended Data Fig. 4f), confirming the requirement of *BBM1–BBM3* genes for seed viability.

To test whether the parent of origin affects seed viability, we performed reciprocal crosses of *BBM1/bbm1 bbm2/bbm2 bbm3/bbm3* to *BBM1/BBM1 bbm2/bbm2 bbm3/bbm3* plants. When the mutant *bbm1* allele was provided by the male parent, approximately 31% of the *bbm1/BBM1* progeny seeds failed to germinate (Extended Data Table 1c), whereas all progeny germinated when the *bbm1* allele was inherited from the female parent (Extended Data Table 1d). Thus,

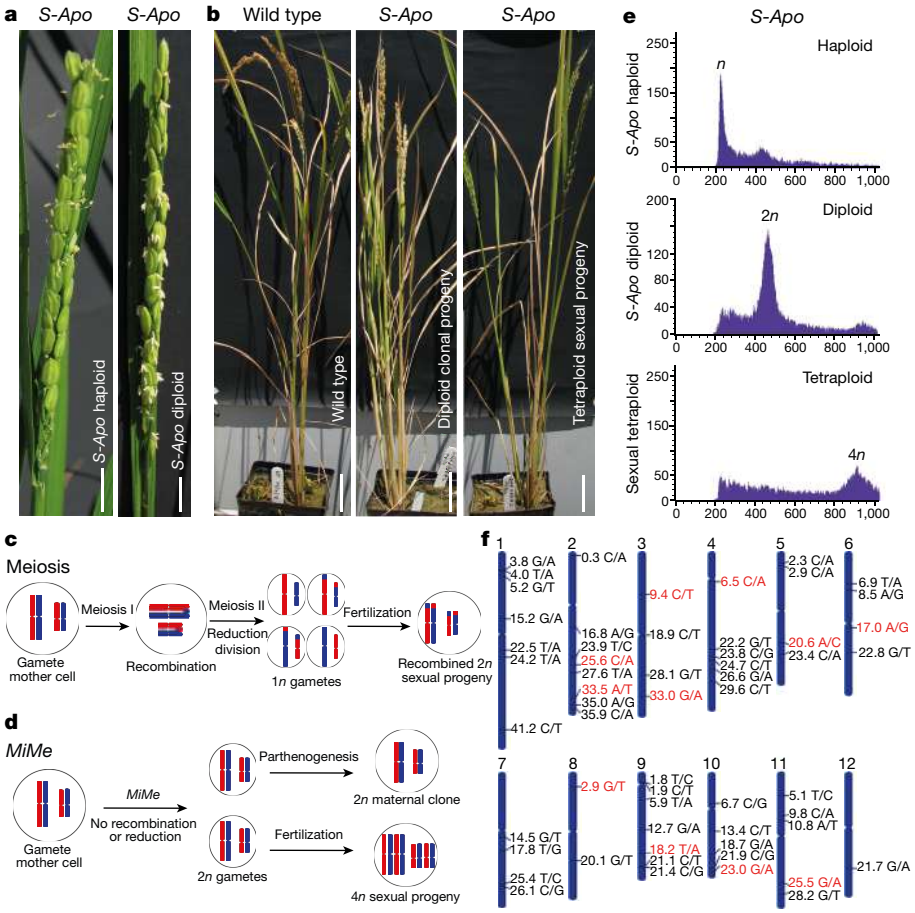

Fig. 3 | Characterization of asexually derived (apomictic) haploids and diploids. a, An *S-Apo* haploid (left; $n = 45$) and *S-Apo* diploid (right; $n = 57$) panicle undergoing anthesis. Scale bars, 1 cm. **b**, Comparison of wild-type (left), *S-Apo* diploid (middle; $n = 57/381$) and sexual tetraploid (right; $n = 324/381$) progeny plants. Scale bars, 5 cm. **c**, **d**, Schematics showing the difference between natural meiosis and *MiMe*. Whereas meiosis and fertilization produce recombined haploid gametes and diploid progeny, *MiMe* leads to the formation of diploid gametes that are clones of the mother plant. Parthenogenesis of a diploid egg cell produces clonal progeny and fertilization of diploid gametes leads to 4*n* sexual progeny. **e**, Flow-cytometric DNA histograms for ploidy determination of *S-Apo* plants. An *S-Apo* haploid (1*n*, top, $n = 30$), an *S-Apo* diploid progeny of a diploid *S-Apo* parent showing a 2*n* peak (middle; $n = 26$) and a sexual tetraploid progeny of a diploid *S-Apo* parent shows a 4*n* peak (bottom; $n = 90$). The *x* axis is the measure of relative fluorescence and the *y* axis shows the number of nuclei. **f**, Chromosomal view showing 57 heterozygous SNPs (position in Mb) identified in the T_0 *S-Apo* mother plant of line 1. The SNPs labelled in red are those additionally confirmed by PCR.

seed viability depends upon a functional *BBM1* allele from the male parent, consistent with male-specific expression of *BBM1* in zygotes. Next we investigated the embryo phenotypes of *bbm2 bbm3* progeny seeds segregating for the *bbm1* mutation. The *bbm1 bbm2 bbm3* embryos were either arrested early or underwent growth by cell division without any corresponding developmental patterning (Fig. 2a). By contrast, embryos that were heterozygous (*BBM1/bbm1 bbm2/bbm2 bbm3/bbm3*) showed a range of phenotypes—from normal to delayed development (Fig. 2b)—as well as the early arrest or unstructured growth phenotypes observed in the triple mutant (Fig. 2b, Extended Data Fig. 4g). This range of phenotypes might occur by partial rescue from late expression of the female *BBM1* allele. Additionally, *BBM4* (Os04g42570)—a fourth *BBM*-like gene that also shows detectable expression in male gametes (Extended Data Table 1a)—might provide sufficient residual function for partial rescue. The recovery of around 0.7% of the *bbm1 bbm2 bbm3* triple homozygous plants is consistent with the hypothesis of residual *BBM* function being provided by *BBM4* (Extended Data Table 1b).

Together, these data suggest that male-genome-derived expression of *BBM1*—acting redundantly with other *BBM* genes—triggers the embryonic program in the fertilized egg cell. Subsequent activation of expression of the female *BBM1* allele by the male BBM1 results in biallelic expression, with both parental alleles eventually contributing to embryo patterning and organ morphogenesis (Fig. 2c). *BBM*-like genes have been shown to promote regeneration from tissue culture, suggesting that they act as pluripotency factors[20]. Our study supports a model in which the requirement of fertilization to initiate embryogenesis in rice arises from the dependency of the zygote on the male gamete for the expression of pluripotency factors after fertilization. This is in contrast to embryogenesis in vertebrate animals, in which pluripotency factors are maternally provided[7]. As demonstrated below, the requirement for fertilization can therefore be bypassed by driving the expression of one such factor from the female gamete.

Haploid plants are efficient tools for the acceleration of plant breeding, because homozygous isogenic lines can be produced in one generation after chromosome doubling[21]. The expression of *BBM1* in the egg cell initiated parthenogenesis in emasculated flowers (Fig. 1b), but the seeds aborted in the absence of endosperm (Extended Data Fig. 3d). Self-pollinated T_1 progeny from *BBM1*-ee transgenic plants were analysed to determine whether endosperm development by fertilization could produce viable seeds containing parthenogenetically derived haploid embryos. We identified haploids by their small size compared with their diploid siblings, as well as by their sterile flowers owing to defective meiosis[22] (Fig. 2d, e, Extended Data Fig. 5a–d). The ploidy of haploid T_1 plants was confirmed by flow cytometry (Fig. 2f). The haploid induction frequency was 5–10% (T_1 plants) and reached around 29% in homozygous T_2 line 8C—this frequency was maintained through multiple generations (Extended Data Table 2a). Thus, misexpression of

the wild-type *BBM1* gene in the egg cell is sufficient for the production of haploid plants.

Crop yields can be improved markedly by the use of F_1 hybrid plants that exhibit enhanced vigour ('hybrid vigour'). If meiosis and fertilization are bypassed, hybrids could be propagated through seeds without segregation. Asexual propagation through seeds—known as apomixes—is known to occur naturally in more than 400 species, although not in the major crop plants[23,24]. The development of a method to introduce apomixis into crop plants has been described as 'the holy grail of agriculture'[5] as it can enable fixation of hybrid vigour and stabilization of superior heterozygous genotypes in breeding programs[6,25]. A genetic approach called *MiMe*, which eliminates recombination and substitutes mitosis for meiosis (Fig. 3c, d), has been reported in *Arabidopsis*[3] and rice[4]. In *MiMe*, a triple knockout of the meiotic genes *REC8*, *PAIR1* and *OSD1* produces unrecombined diploid male and female gametes. We tested the possibility that *BBM1*-ee-induced parthenogenesis in rice combined with *MiMe* could result in asexual propagation through seeds (Extended Data Fig. 5f). The three rice *MiMe* genes[4] were subject to genome editing by CRISPR–Cas9 in haploid and diploid plants carrying the *BBM1*-ee transgene (Extended Data Fig. 6a). Unlike *BBM1-ee* haploids, the *MiMe* + *BBM1*-ee haploids were fertile (Extended Data Fig. 6c, d) with normal anther development (Fig. 3a), suggesting that meiosis was successfully replaced by mitosis. Self-pollination of *MiMe* plants invariably results in doubling of the chromosome number[22], so the progeny of haploid *MiMe* plants should be diploid (double haploid). However, we obtained haploid progeny from two *MiMe* + *BBM1*-ee (hereafter denoted *S-Apo*, for *Synthetic-Apomictic*) haploid mother plants at frequencies of 26% and 15%, due to parthenogenesis (Fig. 3e, top, Extended Data Table 2b). These haploid induction frequencies were maintained for the next two generations (Extended Data Table 2b). These results show that haploid *S-Apo* plants can be propagated asexually through seeds. Additionally, the sexual T_1 double-haploid ($2n$) progeny from the haploid *S-Apo* plants yielded both diploid and tetraploid plants in the T_2, T_3 and T_4 generations; the former class is expected from the successful asexual propagation of double haploids (Extended Data Table 2b).

For the clonal propagation of diploid *S-Apo* plants, we obtained two fertile transformants with the requisite six null mutations in three *MiMe* genes (Extended Data Fig. 7a, b). Diploid *MiMe* rice plants have been previously shown—despite reduced seed sets—to produce exclusively tetraploid progeny by sexual reproduction and no diploids[4] (Extended Data Fig. 6c). However, we obtained diploids at frequencies of 11% and 29% (Extended Data Table 2b) from the progeny of two diploid *S-Apo* (that is, *MiMe* + *BBM1*-ee) T_0 transformants (Fig. 3b–e, Extended Data Fig. 6e). The rest of the progeny were tetraploid (Fig. 3e). The progeny of a control *MiMe* diploid plant were all determined to be tetraploid (Extended Data Fig. 6b, c). Because T_1 diploid progeny of T_0 diploid *S-Apo* parents are predicted to arise from the parthenogenesis of unreduced female gametes, they should be clonal with the parent and should not exhibit genetic segregation. The T_1 diploids were propagated, and two more generations (T_2 and T_3) of diploid clones were identified by flow cytometry screening.

To demonstrate clonal propagation, we performed whole-genome sequencing on a diploid T_0 *S-Apo* mother plant (line 1), two diploid T_1 progeny, two T_2 diploid progeny of diploid T_1 plants and a control untransformed wild-type plant. Analysis for sequence variants identified 57 heterozygous SNPs in unique sequences distributed over the genome in the T_0 mother plant (Fig. 3f, Supplementary Table 1) that are non-variant in the wild-type plant (see Methods). These 57 SNPs were determined to be heterozygous in all four T_1 and T_2 diploid progeny sequenced. The probability of any single progeny retaining heterozygosity by random segregation for just a subset of 22 unlinked SNPs on different chromosome arms is $P = 2.4 \times 10^{-7}$. The maintenance of heterozygosity at all 57 loci for two generations confirms that the diploid progeny are clonally generated by asexual reproduction. The T_0 *S-Apo* mother (line 1) is additionally biallelic for mutations in the *PAIR1* and *REC8* genes, as were all T_1, T_2 and two T_3 diploid progeny tested (Extended Data Fig. 7a). For SNP validation, 11 randomly selected SNPs were amplified by PCR followed by Sanger sequencing[26] and found to be conserved in the T_0 mother plant and all the T_1, T_2 and T_3 progeny tested (Extended Data Fig. 8). The second diploid *S-Apo* transformant (line 5) is biallelic for all three *MiMe* genes (Extended Data Fig. 7b) and also heterozygous for one of the 11 SNPs confirmed by PCR for line 1. Five T_1 diploid progeny carried an identical set of alleles to the T_0 mother (Extended Data Fig. 7b). The probability that all five progeny would inherit heterozygosity at these four loci by random segregation is $P = 1.8 \times 10^{-5}$. These findings from an independently generated apomictic parent provide further support for successful clonal propagation.

This study demonstrates that asexual propagation without genetic segregation can be engineered in a sexually reproducing plant, and illustrates the feasibility of clonal propagation of hybrids through seeds in rice. Seed formation in this system still requires fertilization to make endosperm (Extended Data Fig. 5f). This endosperm is expected to be hexaploid owing to fertilization of a tetraploid central cell by a diploid sperm cell, whereas the parthenogenetic embryo is diploid, giving a 3:1 ploidy ratio. This deviation from the normal 3:2 ploidy ratio of endosperm to embryo does not appear to be consequential for viability or seed size (Extended Data Fig. 6f, g). Additionally, the clonally propagated seeds preserve the 2:1 maternal-to-paternal genome ratio in endosperm that is required for seed viability[27,28]. To engineer a completely asexual system involving autonomous endosperm formation may not be straightforward in a sexually reproducing crop, and nor is it essential, as many natural apomicts also form seeds with fertilized endosperm[23]. The efficiency of clonal propagation in our system is in part limited by the frequency of parthenogenesis, which could potentially be improved in the future, for example with different promoters. An important factor to consider for future rice-breeding strategies is that genome-wide heterozygosity may be less critical for yield than the incorporation of specific alleles that exhibit full or partial dominance[29,30]. Nevertheless, hybrids can provide a rapid route to higher yields from favourable gene combinations, and have been extensively exploited in maize. Because homologous *BBM*-like and *MiMe* genes are found in other cereal crops, including maize[2,20], the methods described here for asexual propagation through synthetic apomixis should be generally extendible to most cereal crops.

Online content

Any methods, additional references, Nature Research reporting summaries, source data, statements of data availability and associated accession codes are available at https://doi.org/10.1038/s41586-018-0785-8.

Received: 8 June 2018; Accepted: 29 October 2018;
Published online 12 December 2018.

1. Palovaara, J., de Zeeuw, T. & Weijers, D. Tissue and organ initiation in the plant embryo: a first time for everything. *Annu. Rev. Cell Dev. Biol.* **32**, 47–75 (2016).
2. Horstman, A., Willemsen, V., Boutilier, K. & Heidstra, R. AINTEGUMENTA-LIKE proteins: hubs in a plethora of networks. *Trends Plant Sci.* **19**, 146–157 (2014).
3. d'Erfurth, I. et al. Turning meiosis into mitosis. *PLoS Biol.* **7**, e1000124 (2009).
4. Mieulet, D. et al. Turning rice meiosis into mitosis. *Cell Res.* **26**, 1242–1254 (2016).
5. Sailer, C., Schmid, B. & Grossniklaus, U. Apomixis allows the transgenerational fixation of phenotypes in hybrid plants. *Curr. Biol.* **26**, 331–337 (2016).
6. Vielle Calzada, J.-P., Crane, C. F. & Stelly, D. M. Apomixis—the asexual revolution. *Science* **274**, 1322–1323 (1996).
7. Lee, M. T., Bonneau, A. R. & Giraldez, A. J. Zygotic genome activation during the maternal-to-zygotic transition. *Annu. Rev. Cell Dev. Biol.* **30**, 581–613 (2014).
8. Nodine, M. D. & Bartel, D. P. Maternal and paternal genomes contribute equally to the transcriptome of early plant embryos. *Nature* **482**, 94–97 (2012).
9. Autran, D. et al. Maternal epigenetic pathways control parental contributions to *Arabidopsis* early embryogenesis. *Cell* **145**, 707–719 (2011).
10. Del Toro-De León, G., García-Aguilar, M. & Gillmor, C. S. Non-equivalent contributions of maternal and paternal genomes to early plant embryogenesis. *Nature* **514**, 624–627 (2014).
11. Anderson, S. N. et al. The zygotic transition is initiated in unicellular plant zygotes with asymmetric activation of parental genomes. *Dev. Cell* **43**, 349–358. e4, (2017).
12. Kim, S., Soltis, P. S., Wall, K. & Soltis, D. E. Phylogeny and domain evolution in the *APETALA2*-like gene family. *Mol. Biol. Evol.* **23**, 107–120 (2006).

13. Boutilier, K. et al. Ectopic expression of BABY BOOM triggers a conversion from vegetative to embryonic growth. *Plant Cell* **14**, 1737–1749 (2002).
14. Passarinho, P. et al. BABY BOOM target genes provide diverse entry points into cell proliferation and cell growth pathways. *Plant Mol. Biol.* **68**, 225–237 (2008).
15. Anderson, S. N. et al. Transcriptomes of isolated *Oryza sativa* gametes characterized by deep sequencing: evidence for distinct sex-dependent chromatin and epigenetic states before fertilization. *Plant J.* **76**, 729–741 (2013).
16. Conner, J. A., Mookkan, M., Huo, H., Chae, K. & Ozias-Akins, P. A parthenogenesis gene of apomict origin elicits embryo formation from unfertilized eggs in a sexual plant. *Proc. Natl Acad. Sci. USA* **112**, 11205–11210 (2015).
17. Conner, J. A., Podio, M. & Ozias-Akins, P. Haploid embryo production in rice and maize induced by *PsASGR-BBML* transgenes. *Plant Reprod.* **30**, 41–52 (2017).
18. Steffen, J. G., Kang, I. H., Macfarlane, J. & Drews, G. N. Identification of genes expressed in the *Arabidopsis* female gametophyte. *Plant J.* **51**, 281–292 (2007).
19. Ohnishi, Y., Hoshino, R. & Okamoto, T. Dynamics of male and female chromatin during karyogamy in rice zygotes. *Plant Physiol.* **165**, 1533–1543 (2014).
20. Lowe, K. et al. Morphogenic regulators *Baby boom* and *Wuschel* improve monocot transformation. *Plant Cell* **28**, 1998–2015 (2016).
21. Murovec, J. & Bohanec, B. in *Plant Breeding* (ed. Abdurakhmonov, I. Y.) Ch. 5 (IntechOpen, London, 2012).
22. Cifuentes, M., Rivard, M., Pereira, L., Chelysheva, L. & Mercier, R. Haploid meiosis in *Arabidopsis*: double-strand breaks are formed and repaired but without synapsis and crossovers. *PLoS ONE* **8**, e72431 (2013).
23. Hand, M. L. & Koltunow, A. M. The genetic control of apomixis: asexual seed formation. *Genetics* **197**, 441–450 (2014).
24. Ozias-Akins, P. & van Dijk, P. J. Mendelian genetics of apomixis in plants. *Annu. Rev. Genet.* **41**, 509–537 (2007).
25. Khush, G. S. *Apomixis: exploiting hybrid vigor in rice*. (International Rice Research Institute, 1994).
26. Sanger, F., Nicklen, S. & Coulson, A. R. DNA sequencing with chain-terminating inhibitors. *Proc. Natl Acad. Sci. USA* **74**, 5463–5467 (1977).
27. Lafon-Placette, C. & Köhler, C. Endosperm-based postzygotic hybridization barriers: developmental mechanisms and evolutionary drivers. *Mol. Ecol.* **25**, 2620–2629 (2016).
28. Sekine, D. et al. Dissection of two major components of the post-zygotic hybridization barrier in rice endosperm. *Plant J.* **76**, 792–799 (2013).
29. Hua, J. et al. Single-locus heterotic effects and dominance by dominance interactions can adequately explain the genetic basis of heterosis in an elite rice hybrid. *Proc. Natl Acad. Sci. USA* **100**, 2574–2579 (2003).
30. Huang, X. et al. Genomic architecture of heterosis for yield traits in rice. *Nature* **537**, 629–633 (2016).

Acknowledgements We thank U. Vijayraghavan for providing pUN and pUGN vectors; S. Kappu, Z. Liechty and C. Santos-Medellín for advice and help with flow cytometry and sequence analysis; B. Van Bockern for rice transformations; and B. Nguyen and A. Yalda for technical assistance, including genotyping and transplantation. This research was supported by research grants from the National Science Foundation (NSF) (IOS-1547760) and the Innovative Genomics Institute to V.S., NSF grant IOS-1810468 to B.Y., National Institutes of Health grant 1S10OD010786-01to the University of California-Davis Genome Center, and by the United States Department of Agriculture Agricultural Experiment Station (project number CA-D-XXX-6973-H). R.M. acknowledges support from the LabEx Saclay Plant Sciences-SPS (ANR-10-LABX-0040-SPS) to the Institut Jean-Pierre Bourgin.

Reviewer information *Nature* thanks T. Dresselhaus and the other anonymous reviewer(s) for their contribution to the peer review of this work.

Author contributions V.S. and I.K. designed the study. I.K. performed experiments and analysed data. D.S. performed analysis of the genome sequences. B.Y. provided pENTR-sgRNA and pUbi-Cas9 vectors for genome editing. V.S. and I. K. wrote the manuscript with input from R.M.

Competing interests The University of California-Davis has filed a patent application on haploid production (PCT/US2017/063249) and a provisional patent application on synthetic apomixis (US62/678,169) arising from this work. INRA has filed a patent application on the use of the MiMe system (EP2208790). The authors declare no other competing interests.

Additional information
Extended data is available for this paper at https://doi.org/10.1038/s41586-018-0785-8.
Supplementary information is available for this paper at https://doi.org/10.1038/s41586-018-0785-8.
Reprints and permissions information is available at http://www.nature.com/reprints.
Correspondence and requests for materials should be addressed to V.S.
Publisher's note: Springer Nature remains neutral with regard to jurisdictional claims in published maps and institutional affiliations.

METHODS

Data reporting. No statistical methods were used to predetermine sample size. The experiments were not randomized and the investigators were not blinded to allocation during experiments and outcome assessment.

Plant materials and growth conditions. Rice cultivar Kitaake (*O. sativa* L. subsp. *japonica*) was used for transformations for raising transgenic lines and as a wild-type control. Wild-type, mutant and transgenic seeds were germinated on half-strength Murashige and Skoog's (MS) medium[31] containing 1% sucrose and 0.3% phytagel in a growth chamber for 12 days, under a 16 h light:8 h dark cycle at 28 °C and 80% relative humidity. Seedlings were then transferred to a greenhouse and grown under natural light conditions in Davis, California.

Chemical treatments. Two-week-old wild-type and *BBM1-GR* seedlings were treated with 0.1% ethanol as mock, 10 μM DEX (Sigma-Aldrich), or 10 μM CYC (Sigma-Aldrich) alone or in combination with 10 μM DEX in liquid half-strength MS[31] salts. Seedlings that were of a similar size and had the same number of leaves were selected for the treatments. Individual biological replicates were constructed using similar leaf samples collected from four different plants, collected for RNA isolation after 24 h. CYC treatments were started 30 min before the DEX treatment in the samples that were treated with both reagents.

Plasmid constructs. Full-length coding sequence (CDS) of *BBM1* was amplified from cDNAs made from rice calli using two sets of primers (KitB1F1 5′-CGGATCCATGGCCTCCATCACC-3′, KitB1R1 5′-CCTTCGACCCCA TCCCAT-3′ and KitB1F2 5′-GGATGGGATGGGGTCGAAG-3′, KitB1R2 3′-GGTACCAGACTGAGAACAGAGGC-3′). The two fragments were fused together by an overlap PCR. The overexpression construct (*BBM1*-ox) was created by cloning *BBM1* coding sequence in pUN vector[32] (Extended Data Fig. 1a). To create the BBM1–GR plasmid (Extended Data Fig. 1e), *BBM1* coding sequence without the stop codon was cloned in pUGN vector[32] for translational fusion with rat glucocorticoid receptor[33]. The whole *BBM1* locus, approximately 3kb upstream sequences and the transcribed region until the stop codon were PCR-amplified in two fragments from genomic DNA using two primer pairs: pB1F1 5′-CTCGAGGTCAACACCAACGCCATC-3′, pB1R1 5′- GAAGTCCTCCAGCTTCGGCGC-3′ and pB1F2 5′-TTGATTGTGTTGATG TGCAGAGTGGGG-3′, pB1R2 5′-CTCGAGCGGTGTCGGCAAAACC-3′. The two fragments were joined at a unique restriction enzyme site, NotI, present downstream of the start codon in the sequence. The whole locus was moved to a pCAMBIA1300 vector already containing *Arabidopsis* histone H2B, eGFP and nopaline synthase gene terminator (Extended Data Fig. 2b). The construct for egg-cell-specific expression of BBM1 was made by cloning *BBM1* downstream to *Arabidopsis* DD45 promoter[18] and upstream of the nopaline synthase terminator (Extended Data Fig. 3b) in pCAMBIA1300.

For genome editing of *BBM1*, *BBM2* and *BBM3* genes, single-guide RNA (sgRNA) sequences 5′-GGAGGACTTCCTCGGCATGC-3′, 5′-GTATGCAATATACTCCTGCC -3′ and 5′-GACGGCGGGAGCTGATCCTG -3′, respectively, were designed by using the web tool https://www.genome.arizona.edu/crispr/ as described[34]. The sgRNAs were cloned in pENTR-sgRNA entry vector. The binary vectors for plant transformations (pCRISPR *BBM1* + *BBM3*, pCRISPR *BBM2* + *BBM3* and pCRISPR *BBM1* + *BBM2* + *BBM3*) were constructed by Gateway LR clonase (Life Technologies) recombination with pUbi–Cas9 destination vector as described[35]. Three candidate genes (*OSD1*, Os02g37850; *PAIR1*, Os03g01590 and *REC8*, Os05g50410) for creating *MiMe* mutations in rice were selected as previously described[4] and sgRNAs sequences 5′-GCGCTCGCCGACCCCTCGGG-3′, 5′-GGTGAG GAGGTTGTCGTCGA-3′ and 5′-GTGTGGCGATCGTGTACGAG-3′, respectively, for CRISPR–Cas9-based knockout were designed as described[34]. Vector pCAMBIA2300 *MiMe* CRISPR–Cas9 (Extended Data Fig. 6a) for plant transformations was constructed as described[35], except the resistance marker in the destination vector pUbi–Cas9 was changed to kanamycin (*Neomycin Phosphotransferase II*). pCAMBIA2300 *MiMe* CRISPR–Cas9 was transformed in embryogenic calli derived from *pDD45::BBM1#8c* haploid inducer lines (Extended Data Fig. 3b). Rice transformations were carried out as previously described[36] at the University of California-Davis plant transformation facility. T_0 plants were grown in a greenhouse and screened for *MiMe* mutations. T_1 plants obtained from seeds were subjected to ploidy determination and genotyping for *MiMe* mutations.

Generating *bbm1 bbm2 bbm3* mutants. Rice embryogenic calli were transformed with pCRISPR *BBM1* + *BBM3*, or pCRISPR *BBM2* + *BBM3*. The transformants that carried the *bbm1 bbm3* and *bbm2 bbm3* double mutations generated by genome editing (Extended Data Fig. 4a, b) did not show any phenotypic abnormalities and were fertile. The two double mutants were crossed and selfed; however, no *bbm1 bbm2 bbm3* triple-homozygous plants were recovered in the F_2 generation (Extended Data Fig. 4c). However, plants heterozygous for *BBM1 (bbm1/BBM1)* but homozygous mutant for both *bbm2* and *bbm3* could be recovered, and their progeny were analysed in detail (Extended Data Fig. 4d).

Genotyping. Genotyping of *BBM1*, *BBM2* and *BBM3* mutants was carried out by PCR-amplifying DNA at the mutation site with primers *BBM1* SeqF 5′-TTGATTGTGTTGATGTGC-3′ *BBM1* SeqR 5′-GAGAGACGACCTACTTG GTGAC-3′; *BBM2* SeqF 5′-TAGCTAGCTTGTTAATAGATCATAG-3′, *BBM2* SeqR 5′-TCATATCTCAGTGTGATAGTCTG-3′; and *BBM3* SeqF 5′-ATGCTGCTGCTCCGAGAAG-3′, *BBM3* SeqR 5′-GCTTAGTGCTCCAAACCTCTC-3′. Sanger sequencing[26] of the three PCR amplicons of 464 bp, 262 bp and 547 bp, respectively, for the three genes was carried out at the University of California-Davis DNA-sequencing facility. Because a 1-bp deletion mutation in *BBM1* disrupted an SphI restriction-enzyme site (Extended Data Fig. 4d), all further genotyping of *BBM1* for mutational analysis was performed with restriction digestion of the PCR amplicon with SphI (Extended Data Fig. 4e). For genotyping developing seeds of 5 DAP onwards, endosperm was used for genotyping and embryos were collected for mutant phenotype analysis. DNA fragments at the mutation sites of three *MiMe* genes were PCR-amplified with primers *OSD1* F 5′-TTACTTGGAAGAGGCAGGAGCC -3′, *OSD1* R 5′-ACCTTGACGACTGACGTGATGTC-3′; *PAIR1* F 5′-GTGG TGTGGTGTGTTCAGGAG-3′, *PAIR1* R 5′-TGGAATCCCCAA TCAGTAAGGCAC-3′; and *REC8* F 5′-GCACTAAGGCTCTCCGGAATTCTC-3′, *REC8* R 5′-AATGGATCAAGGAGGAGGCACC-3′. PCR amplicons of 364 bp, 344 bp and 326 bp—for *OSD1*, *PAIR1* and *REC8*, respectively—were subjected to Sanger sequencing[26] for mutation analysis.

Emasculation, crosses and pollinations. Flowers from *BBM1*-ee T_0 transgenic rice lines were emasculated around the anthesis stage, bagged and allowed to grow for another nine days after emasculation. Carpels were collected and fixed for analysis in formaldehyde (10%)–acetic acid (5%)–ethanol (50%). A translational fusion consisting of the *BBM1* genomic locus to GFP (BBM1–GFP; Extended Data Fig. 2b) was introduced into the inbred *japonica* (Kitaake) cultivar by transformation. Plants hemizygous for the BBM1–GFP transgene were then reciprocally crossed to wild-type plants. Flowers from wild-type or BBM1–GFP transgenic plants were hand-pollinated around the anthesis stage and carpels were collected 2.5 and 6.5 HAP.

For phenotypic analysis of mutant embryos, self-pollinated flowers from mutant plants were scored for anthesis, and collected 5 or 10 DAP. For crosses of *bbm1 bbm3* and *bbm2 bbm3* plants, only T_2 progeny plants in which the CRISPR–Cas9 transgene had already segregated out were used as parents. For all crosses of *bbm1 bbm3* with *bbm2 bbm3* plants, and for the reciprocal crosses between *BBM1/bbm1 bbm2/bbm2 bbm3/bbm3* and *BBM1/BBM1 bbm2/bbm2 bbm3/bbm3* plants, panicles used as females were emasculated and bagged with pollen donor panicles. The bags were gently finger-tapped (twice a day) for the next two days. Male panicles were removed, and female panicles were left bagged to make seeds. F_1 seeds were collected four weeks after pollination.

Immunohistochemistry and toluidine blue staining. Owing to the difficulty of imaging GFP fluorescence in early rice zygotes through the carpel tissue, we used antibodies against GFP to detect zygote expression in sectioned rice carpels. Collected carpels were fixed in formaldehyde (10%)–acetic acid (5%)–ethanol (50%). Tissue embedding and sectioning was performed as described previously[37]. Immunohistochemistry was carried out using standard protocols[38], except an antigen-retrieval step was also included. Antigen retrieval was performed by microwaving the slides in 10 mM sodium citrate buffer (pH 6.0) for 10 min. Rabbit anti-GFP antibody ab6556 (Abcam) was used as the primary antibody and goat anti-rabbit alkaline phosphatase conjugate A9919 (Sigma) was used as the secondary antibody. For toluidine blue staining, after rehydration, sections crosslinked to glass slides were stained with 0.01% toluidine blue for 30 s.

Flow cytometry. Nuclei for fluorescence-activated cell sorting (FACS) analysis were isolated by a leaf-chopping method described previously[39]. The isolated nuclei were stained with propidium iodide at 40 μg ml^{-1} in Galbraith's buffer. FACS analysis and DNA-content estimation was carried out using a Becton Dickinson FACScan system using standard protocols[40,41]. DNA histograms were gated out for the initial debris.

Alexander staining of pollen grains. Stamens were collected just before anthesis. Anthers were put on a glass slide in a drop of Alexander's stain containing 40 μl of glacial acetic acid per millilitre of stain[42]. Anthers were covered with a coverslip and slides were heated at 55 °C on a heating block, until the visible staining of pollen was observed.

Library preparation and sequencing. PCR-free DNA libraries were prepared from a wild-type Kitaake control plant, the T_0 *S-Apo* line 1 mother plant, two T_1 and two T_2 progeny clones from *S-Apo* line 1 with 500 ng of input DNA, using NuGEN Celero DNA-Seq kit, following the manufacturer's instructions. Samples were multiplexed and six libraries per lane were run on Illumina HiSeq platforms at the University of California-Davis Genome Center.

Whole-genome DNA sequencing and statistical analysis. Adaptor removal and quality trimming of 150-bp paired-end reads was performed using Trimmomatic

0.38[43] resulting in 13–16 gigabases of sequence for each library. The reads were aligned to the *O. sativa* reference genome (Nipponbare, Release 7.0)[44] using *bwa mem*[45]. To discover variants that were heterozygous in the T_0 mother plant (line 1), the variant finder GATK4.0 HaplotypeCaller was used in single-sample mode[46] and selecting only for SNPs. Repeated elements of the genome were masked from analysis using annotated repeats from http://www.phytozome.org (Osativa_323_v7.0.repeatmasked_assembly_v7.0.gff3). Variants were retained for analysis after filtering on the basis of mapping quality (MQ = 60), QualByDepth (QD >2), StrandOddsRatio (SOR <1.8), unfiltered read depth ($10 \leq DP \leq 40$) and fraction of the alternate allele ($0.4 \leq DP \leq 0.6$), with the expectation that a truly heterozygous locus should show roughly equal numbers of read counts for each allele. To increase certainty that the set of loci included only true heterozygous SNPs, loci which were called heterozygous in the wild-type sample were also discarded. This strategy guards against instances in which incorrect read-mapping over multi-copy regions lead to spurious designation of loci as heterozygous, even though it is likely that we also discarded true heterozygous loci in the process. A final list of 60 high-quality heterozygous SNPs at 57 loci were analysed for segregation in the four progeny clones (T_1 clone A, T_1 clone B, T_2 clone 7 and T_2 clone 21). All SNPs were called heterozygous by HaplotypeCaller in all the progeny samples (Supplementary Table 1).

For statistical analysis of genetic ratios: Either a chi-square goodness-of-fit test or a two-tailed Fisher's exact test was carried out wherever applicable, and the result specified in the legend of the relevant figure or table.

RT–PCR and RT–qPCR. All the cDNAs were synthesized using the iScript cDNA synthesis kit (BioRad) according to the manufacturer's instructions. RT–PCRs were performed with MyTaq Red Mix (Bioline) and RT–qPCRs with iTaq universal SYBR Green supermix (BioRad) using CFX96 Touch real-time PCR system (BioRad). *UBIQUITIN5* (Os03g13170) was used as the internal control and fold changes in the relative abundance of transcripts were calculated as described previously[47]. For RT–qPCR, amplifications for each gene were performed in two biological replicates, and each biological replicate was repeated in three technical replicates for each sample. For *BBM1*, *BBM1* RT F 5′-TACTACCTTTCCGAGGGTTCG-3′ was used in combination with B1RNAi R 5′-GATATC CCAGACTGAGAACAGAGGC -3′ to detect endogenous transcript and with GR RT R 5′-TCTTGTGAGACTCCTGCAGTG-3′ to detect *BBM1-GR* transgenic transcript in RT–qPCR experiments. *BBM1*intronF 5′-GTGGCAGGAAACAAGGATCTG-3′ with B1RNAi R which spanned an intron was used in RT–PCR experiments. For other genes tested in this study, the following primer combinations were used: *LEC1A* F 5′-GACAGGTGATCGAGCTCGTC-3′, *LEC1A* R 5′-CTCTTTCGATGAAACGGTGGC-3′; *LEC1B* F 5′-ACAGC AGCAGAATGGCGATC-3′, *LEC1B* R 5′-CTCATCGATCACTACCTGAACG-3′; *GE* F 5′-CAGGAGCACAAGGCGAAGCG-3′, *GE* R 5′-CTTCGCCTGGATCT CCGGGTG-3′; *OSH1* F 5′-GAGATTGATGCACATGGTGTG-3′, *OSH1* R 5′-CGAGGGGTAAGGCCATTTGTA-3′; and *UBIQUITIN5* F 5′-ACCACTTCGA CCGCCACT-3′, *UBIQUITIN5* R 5′-ACGCCTAAGCCTGCTGGTT-3′.

SNP analysis. Detection of SNPs in *BBM1* transcripts from hybrid zygotes was performed by PCR of 2.5 HAP zygote cDNAs from reciprocally crossed rice *japonica* cultivar Kitaake and *indica* cultivar IR50, as described previously[11]. Primers B1RNAi F 5′-CCTCGAGCAACTATGGTTCGCAGC-3′ and B1RNAi R, which amplified a gene-specific fragment of about 600 bp of *BBM1*, contains 5 SNPs between Kitaake and IR50 (Extended Data Fig. 2a). The PCR amplicons were Sanger-sequenced[26] and chromatograms were analysed for SNPs. For detection of heterozygous SNPs present in the *S-Apo* mother plants and their progeny, 50 ng of input DNA was used for each PCR reaction. Sanger-sequenced[26] PCR chromatograms were analysed for the presence of SNPs. The primers for 11 SNPs analysed are: 1 Chr2 F 5′-TGGGTGCCA CGTTATCTAGG-3′, 1 Chr2 R 5′-GGATTTGGCTACCCTCAAGCT-3′; 2 Chr2 F 5′-GAATGGGCAACTAACAACCGTG-3′, 2 Chr2 R 5′-ACCGTG GAAAGGAACAGCTG-3′; 1 Chr3 F 5′-TGCTGAAGGTGACGTTGATCTG-3′, 1 Chr3 R 5′-CGACGCCAACGAGAAGGA-3′; 2 Chr3 F 5′-GCTCCAGTGCTA GAGAGACATC-3′, 2 Chr3 R 5′-AGCCACCCAGTAACCGTTG-3′; Chr4 F 5′-GATTGGCAAACCAGCTACTGC-3′, Chr4 R 5′-CTGATGGCAAG CTGTTGGC-3′; Chr5 F 5′-ATGATCTGCTGCTTGTTTCAATGC-3′, Chr5 R 5′-TATCCTTCAAGCACCACTGCC-3′; Chr6 F 5′-ACTAATGGGACCACT TGACAGC-3′, Chr6 R 5′-TCAGCCTGAGATGGCTTGG-3′; Chr8 F 5′-CAGACTGTGGGACGCTACATG-3′, Chr8 R 5′-AGAAGATCT GGGCAGCAGTC-3′; Chr9 F 5′-GCTGCACCTGTTAGCTATGTGA-3′, Chr9 R 5′-AGCATCCCAAAAGCACACATG-3′; Chr10 F 5′-TCAGCAGCCTAAGGTT GAAGG-3′, Chr10 R 5′-CTGCTGCTGCTTCATGATCAC-3′; and Chr11 F 5′-GCAGGAACTATTGCCTCTCATGA-3′, Chr11 R 5′-TCAGTCTCATAGCGCA CCAC-3′.

Code availability. Codes for the different analyses are available for non-commercial use from the corresponding author upon request.

Reporting Summary. Further information on research design is available in the Nature Research Reporting Summary linked to this article.

Data availability

Whole-genome DNA sequencing data for *S-Apo* line 1 mother plant, the four progeny clones from two generations, and the Kitaake wild-type control are available from National Center for Biotechnology Information (NCBI) BioProject number PRJNA496208. RNA sequencing data from previously published datasets[11,15] are available from the NCBI Short Read Archive as Project SRP119200 and from the NCBI Gene Expression Omnibus under accession number GSE50777.

31. Murashige, T. & Skoog, F. A revised medium for rapid growth and bio assays with tobacco tissue cultures. *Physiol. Plant.* **15**, 473–497 (1962).
32. Khanday, I., Yadav, S. R. & Vijayraghavan, U. Rice *LHS1/OsMADS1* controls floret meristem specification by coordinated regulation of transcription factors and hormone signaling pathways. *Plant Physiol.* **161**, 1970–1983 (2013).
33. Aoyama, T. & Chua, N. H. A glucocorticoid-mediated transcriptional induction system in transgenic plants. *Plant J.* **11**, 605–612 (1997).
34. Xie, K., Zhang, J. & Yang, Y. Genome-wide prediction of highly specific guide RNA spacers for CRISPR–Cas9-mediated genome editing in model plants and major crops. *Mol. Plant* **7**, 923–926 (2014).
35. Zhou, H., Liu, B., Weeks, D. P., Spalding, M. H. & Yang, B. Large chromosomal deletions and heritable small genetic changes induced by CRISPR/Cas9 in rice. *Nucleic Acids Res.* **42**, 10903–10914 (2014).
36. Hiei, Y. & Komari, T. Agrobacterium-mediated transformation of rice using immature embryos or calli induced from mature seed. *Nat. Protoc.* **3**, 824–834 (2008).
37. Javelle, M., Marco, C. F. & Timmermans, M. In situ hybridization for the precise localization of transcripts in plants. *J. Vis. Exp.* **57**, e3328 (2011).
38. Sessions, A. Immunohistochemistry on sections of plant tissues using alkaline-phosphatase-coupled secondary antibody. *Cold Spring Harb. Protoc.* https://doi.org/0.1101/pdb.prot4946 (2008).
39. Galbraith, D. W. et al. Rapid flow cytometric analysis of the cell cycle in intact plant tissues. *Science* **220**, 1049–1051 (1983).
40. Doležel, J., Greilhuber, J. & Suda, J. Estimation of nuclear DNA content in plants using flow cytometry. *Nat. Protoc.* **2**, 2233–2244 (2007).
41. Cousin, A., Heel, K., Cowling, W. A. & Nelson, M. N. An efficient high-throughput flow cytometric method for estimating DNA ploidy level in plants. *Cytometry A* **75A**, 1015–1019 (2009).
42. Alexander, M. P. Differential staining of aborted and nonaborted pollen. *Stain Technol.* **44**, 117–122 (1969).
43. Bolger, A. M., Lohse, M. & Usadel, B. Trimmomatic: a flexible trimmer for Illumina sequence data. *Bioinformatics* **30**, 2114–2120 (2014).
44. Kawahara, Y. et al. Improvement of the *Oryza sativa* Nipponbare reference genome using next generation sequence and optical map data. *Rice (N. Y.)* **6**, 4 (2013).
45. Li, H. & Durbin, R. Fast and accurate short read alignment with Burrows–Wheeler transform. *Bioinformatics* **25**, 1754–1760 (2009).
46. Van der Auwera, G. A. et al. From FastQ data to high confidence variant calls: the Genome Analysis Toolkit best practices pipeline. *Curr. Protoc. Bioinformatics* **11**, 11.10.1–11.10.33 (2013).
47. Livak, K. J. & Schmittgen, T. D. Analysis of relative gene expression data using real-time quantitative PCR and the $2^{-\Delta\Delta CT}$ method. *Methods* **25**, 402–408 (2001).

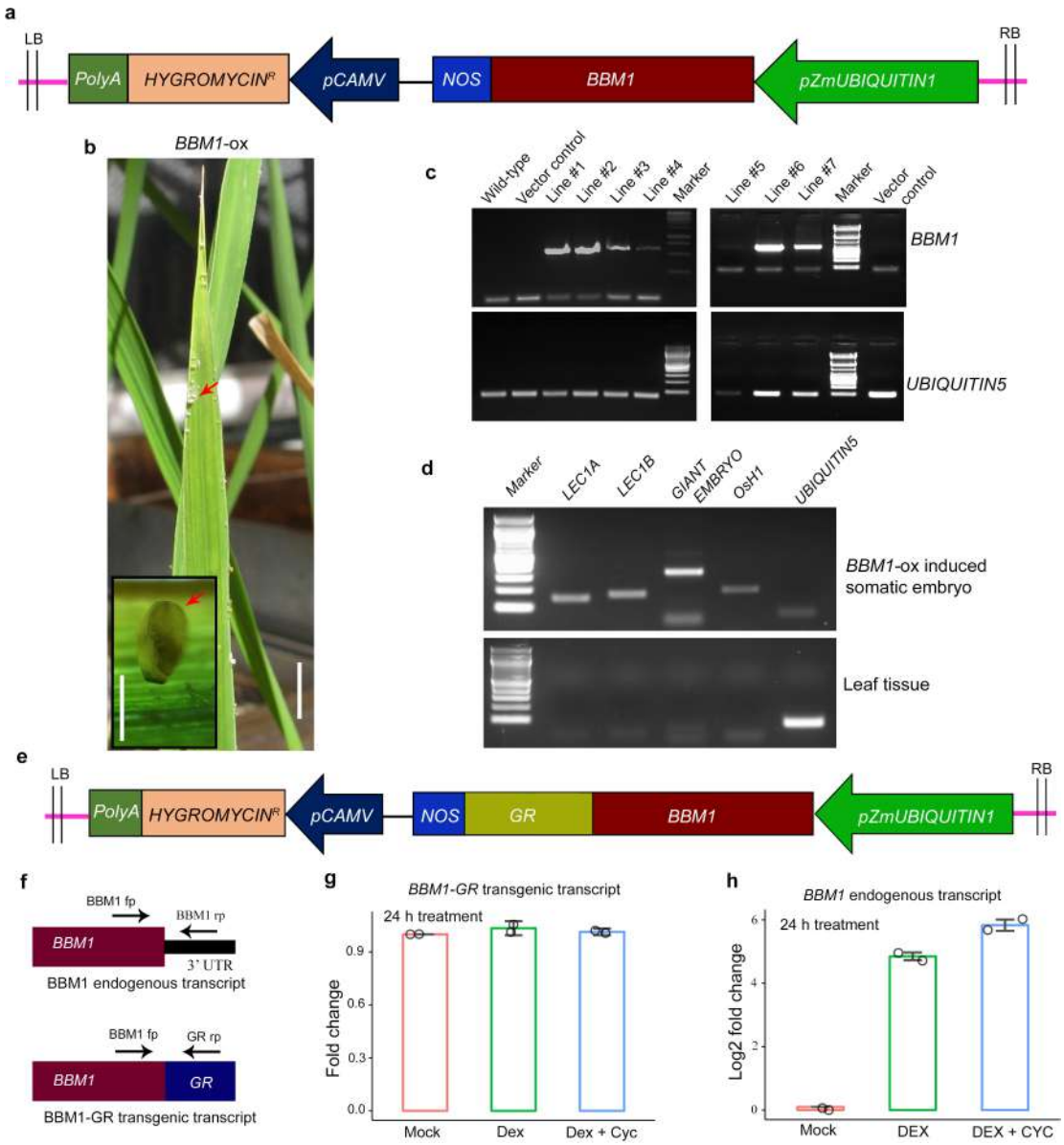

Extended Data Fig. 1 | *BBM1*-induced somatic embryogenesis and auto-activation. a, Schematic of binary construct between T-DNA borders used for ectopic expression (*BBM1*-ox). **b**, Somatic embryo-like structures induced by *BBM1* ectopic expression in rice leaves ($n = 14/20$ transgenic lines). Scale bar, 1 cm. Inset, magnified view of a somatic embryo; scale bar, 0.5 mm. Fourteen of the twenty transgenic plants raised showed the development of such embryo-like structures observed on adult seedlings from the fourth leaf onwards. **c**, Confirmation by RT–PCR of ectopic *BBM1* expression in leaf tissues of transgenic lines. *BBM1* is not expressed in wild-type leaves ($n = 2$ independent replicates). **d**, RT–PCR of embryo marker genes to confirm the embryo identity of somatic embryos induced by *BBM1* overexpression. *OsH1*, *O. sativa HOMEOBOX1*; *LEC1*, *LEAFY COTYLEDON1* ($n = 2$ independent biological replicates). **e**, Schematic of plasmid construct for DEX-inducible BBM1–GR expression system. **f**, Schematic showing primer combinations to distinguish between endogenous *BBM1* and *BBM1-GR* fusion transcripts. **g**, RT–qPCR for fold changes in *BBM1-GR* fusion transcript in samples treated for 24 h with the indicated reagents, showing essentially no differences between treatments. $n = 2$ independent biological replicates (see Methods), data are mean ± s.e.m. and each data point represents the average fold change from three replicates. **h**, Autoactivation of *BBM1* in samples treated with DEX for 24 h, detected by RT–qPCR. $n = 2$ independent biological replicates (see Methods), data are mean ± s.e.m. and each data point represents the average fold change (measured as $\log_2$(change in expression)) from three replicates.

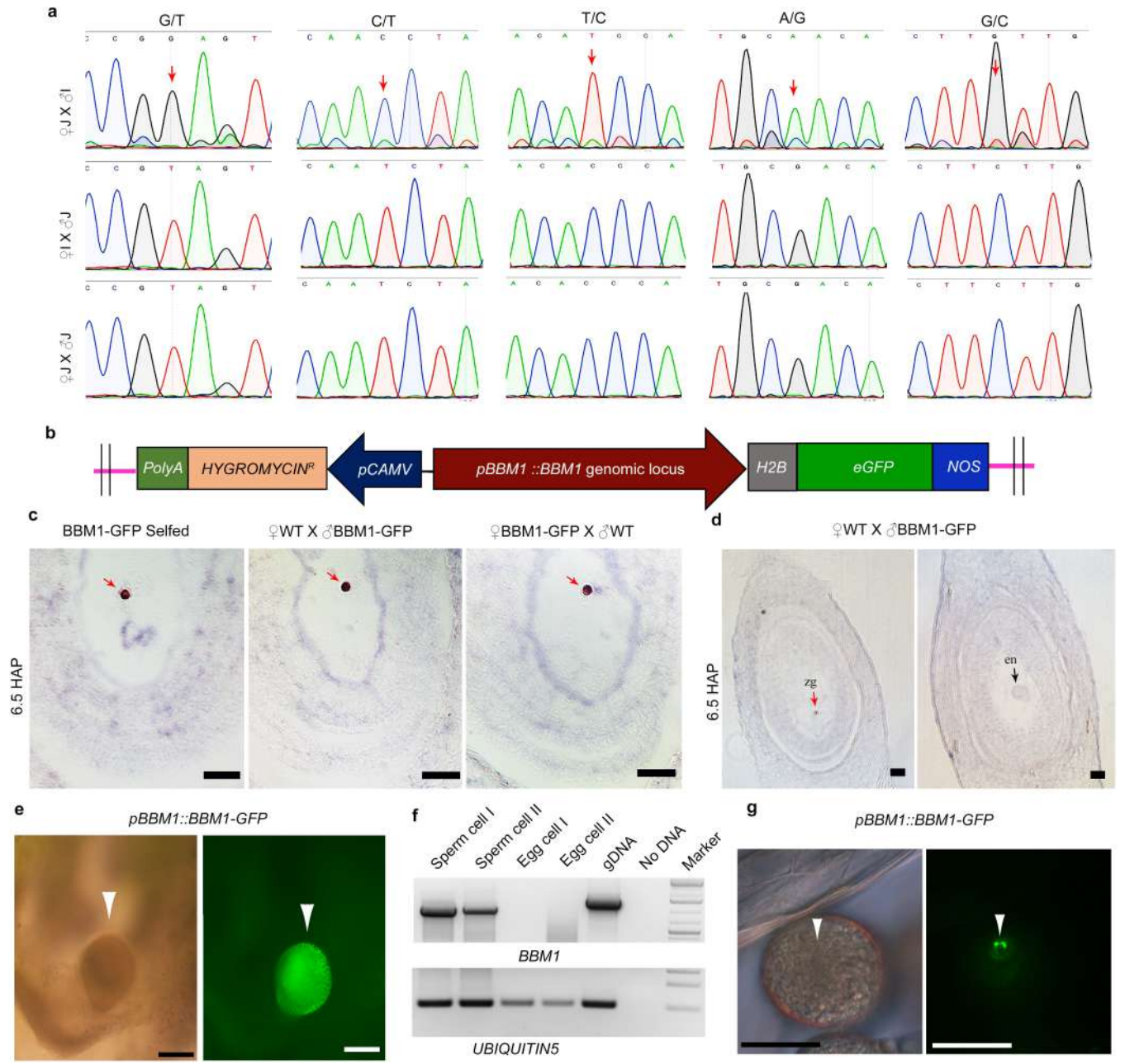

Extended Data Fig. 2 | *BBM1* expression in zygotes and gametes. **a**, Five SNPs sequenced after RT–PCR amplification (red arrows), showing expression only from the male allele in hybrid (J, *japonica*; I, *indica*) 2.5 HAP zygotes ($n = 2$ biological replicates). **b**, Schematic of the *BBM1-GFP* binary construct. **c**, Immunohistochemistry showing expression from both male and female *BBM1* alleles in isogenic 6.5 HAP zygote nuclei ($n = 20$), as compared to male-specific expression at 2.5 HAP (Fig. 1a). Scale bars, 25 μm. **d**, Holistic view of a 6.5 HAP embryo sac showing BBM1–GFP expression in the zygote nucleus (left), while in the same embryo sac expression is not detected in the dividing endosperm (right). zg, zygote. $n = 20$. Scale bar 100 μm. **e**, BBM1–GFP expression in globular-stage rice embryos (white arrowhead, $n = 30$). Differential interference contrast image (left); fluorescence image (right panel). Scale bars, 200 μm. **f**, RT–PCR showing *BBM1* expression in sperm cells; however, the transcript is not detected in egg cells ($n = 2$ independent biological replicates). Primers used for detecting *BBM1* transcript span an intron (see Methods). **g**, BBM1–GFP expression in sperm cells (white arrowhead points to sperm nuclei, $n = 20$). Differential interference contrast image (left) and fluorescent image (right) of a germinating pollen grain showing BBM1–GFP expression in the two sperm cell nuclei.

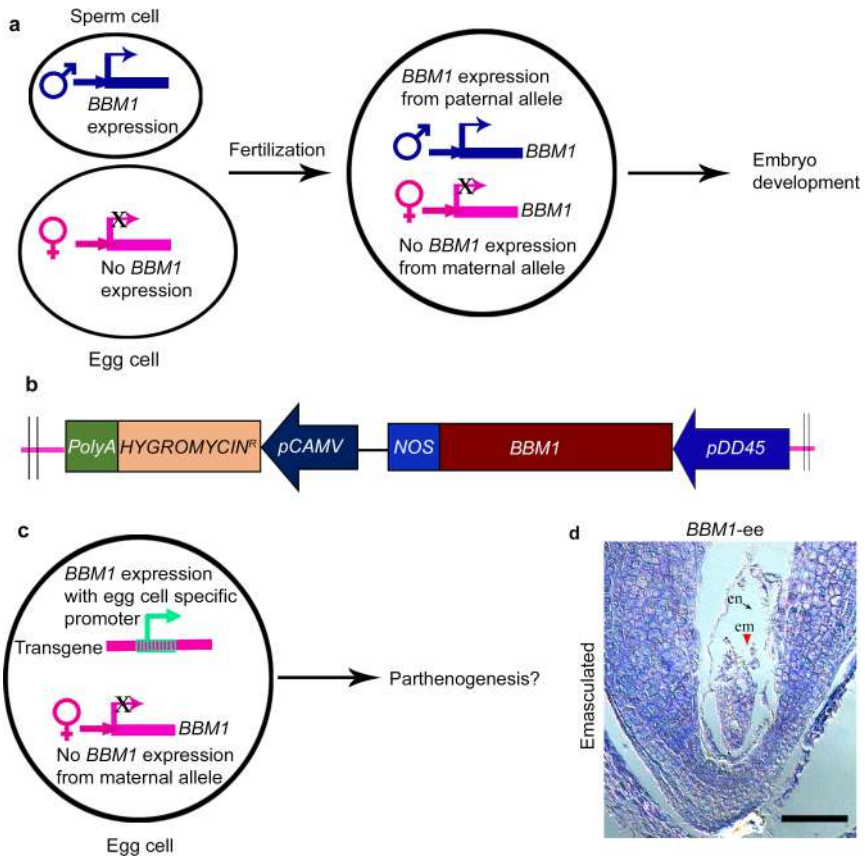

Extended Data Fig. 3 | Parthenogenesis induction by expression of *BBM1* in the egg cell. a, Schematic showing wild-type expression pattern of *BBM1*. **b**, Sketch of T-DNA region of the binary vector used for *BBM1* expression in the egg cell. **c**, Schematic representation of the hypothesis that the expression of *BBM1* in the egg cell can induce parthenogenesis. **d**, A degenerating parthenogenetic embryo (*BBM1*-ee) at 9 days after emasculation (red arrowhead). No endosperm development (black arrow) is observed in emasculated carpels, leading to the abortion of embryos ($n = 12/98$). Scale bar, 100 μm.

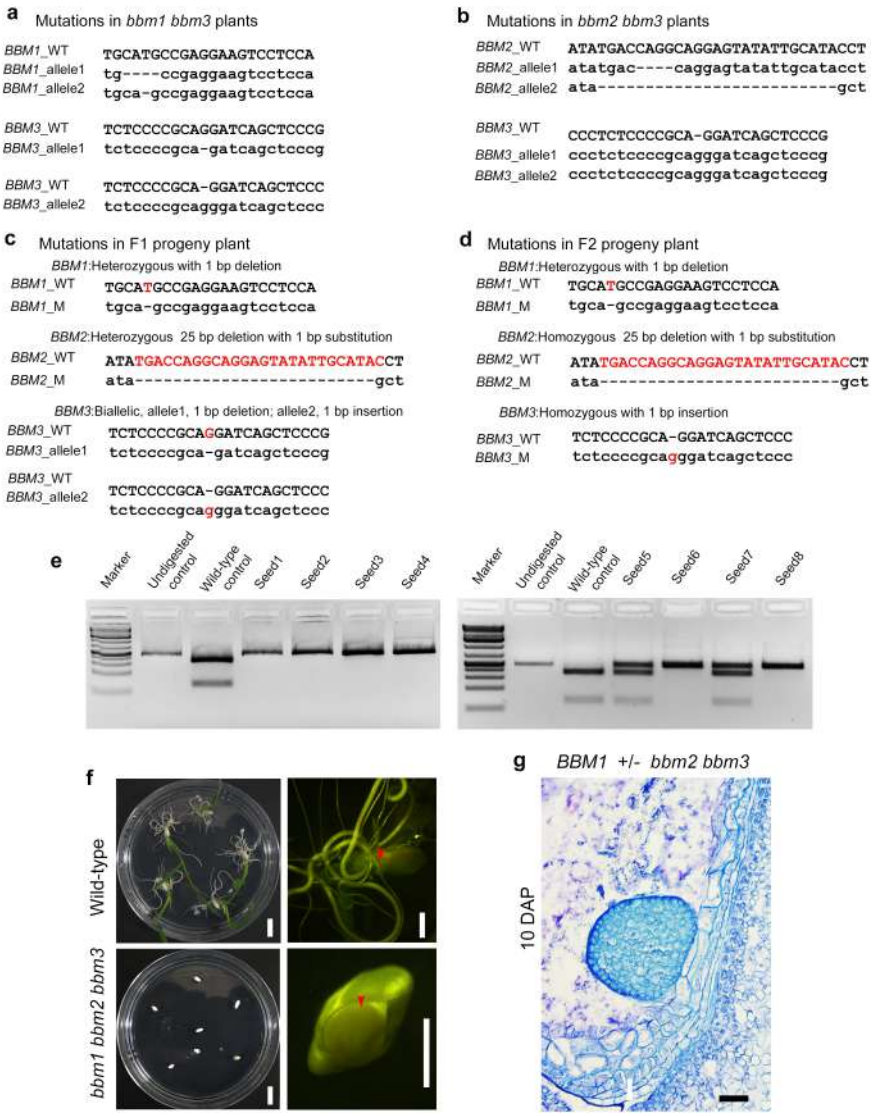

Extended Data Fig. 4 | CRISPR–Cas9 edited mutations in *BBM1*, *BBM2* and *BBM3* in rice. a, DNA sequences of mutations in *bbm1/bbm1 bbm3/bbm3* plants. **b**, DNA sequences of mutations in *bbm2/bbm2 bbm3/bbm3* plants. **a** and **b** were chosen as parents for crosses to generate the *bbm1 bbm2 bbm3* triple homozygous mutants shown in **c** and **d**. **c**, Mutations in the F_1 progeny plant. It is heterozygous for *BBM1* and *BBM2*, and biallelic for *BBM3*. **d**, Mutations in the F_2 progeny plant used for genetic analysis. The plant is heterozygous for *BBM1* with a 1-bp deletion. The *BBM2* locus has a homozygous 25-bp deletion and 1-bp substitution, and the *BBM3* locus is a homozygous mutant with 1-bp insertion. **e**, Genotyping of non-germinating seeds ($n = 8$). The 1-bp deletion mutation in *BBM1* results in disruption of an SphI restriction site. **f**, Seed lethality in *bbm1 bbm2 bbm3* triple homozygous plants. Top, germinating one-week-old wild-type seeds ($n = 30$). Scale bars, 1 cm. A magnified view is shown on the right. Bottom, non-germinating seeds of *bbm1 bbm2 bbm3* triple homozygous plants ($n = 70$). A zoomed-in image of a non-germinating *bbm1 bbm2 bbm3* seed, one week after plating, is shown on the bottom right. No seedling emerged from the embryo site (red arrowhead). **g**, Additional image of a *BBM1/bbm1* heterozygous *bbm2/bbm2 bbm3/bbm3* homozygous 10 DAP embryo ($n = 3/53$) showing no organ formation, similar to triple homozygote phenotype (see Fig. 2a). Scale bar, 100 μm.

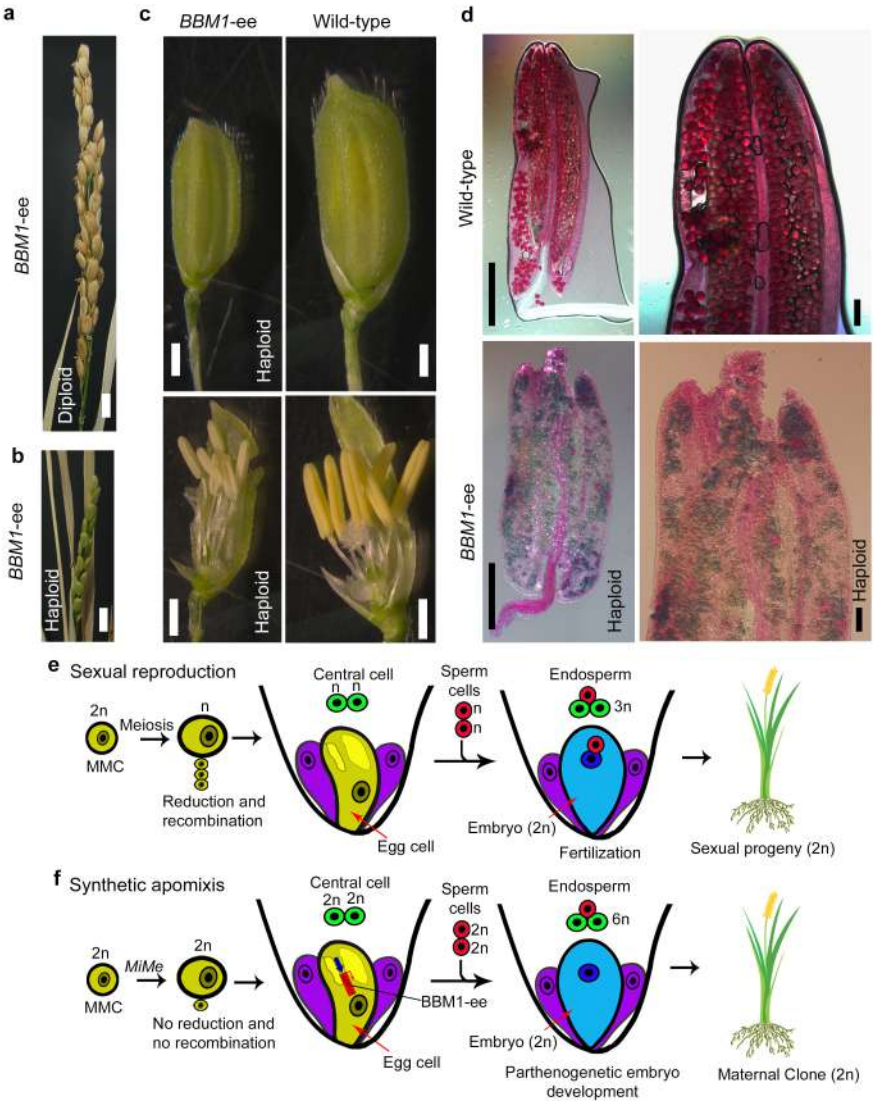

Extended Data Fig. 5 | Haploid induction and synthetic apomixis. Haploids shown are derived from *BBM1*-ee diploids by parthenogenesis. **a**, A control diploid sibling panicle with fertile florets ($n = 442$ plants). Scale bar, 1 cm. **b**, A haploid panicle with infertile florets ($n = 113$ plants). Scale bar, 1 cm. **c**, Differences in floret and floral organ sizes between haploid and control diploid. Left, *BBM1*-ee haploid; right, wild-type control ($n = 20$). Scale bars, 1 mm. **d**, Pollen viability in haploids as assessed by Alexander staining. Top, control wild-type anther with viable pollen ($n = 10$). Bottom, *BBM1*-ee haploid anther with non-viable pollen ($n = 20$). Scale bars, 0.5 mm (left) and 200 μm (right). **e**, **f**, Sexual reproduction compared with asexual reproduction through seed (synthetic apomixis). **e**, Schematic representation of sexual reproduction. Gametes form by meiotic recombination and division; fertilization and gamete fusion give rise to diploid progeny. **f**, Synthetic apomixis. *MiMe* omits meiosis and gives an unrecombined and unreduced ($2n$) egg cell. The $2n$ egg cell is converted parthenogenetically into a clonal embryo by *BBM1*-ee. The endosperm forms in both pathways by fertilization of central cell (homodiploid in wild type, tetraploid in synthetic apomicts) by a sperm cell (haploid in wild type, diploid in synthetic apomicts). The maternal:paternal genome ratio of 2:1 is maintained in the endosperm in both the pathways, ensuring normal seed development.

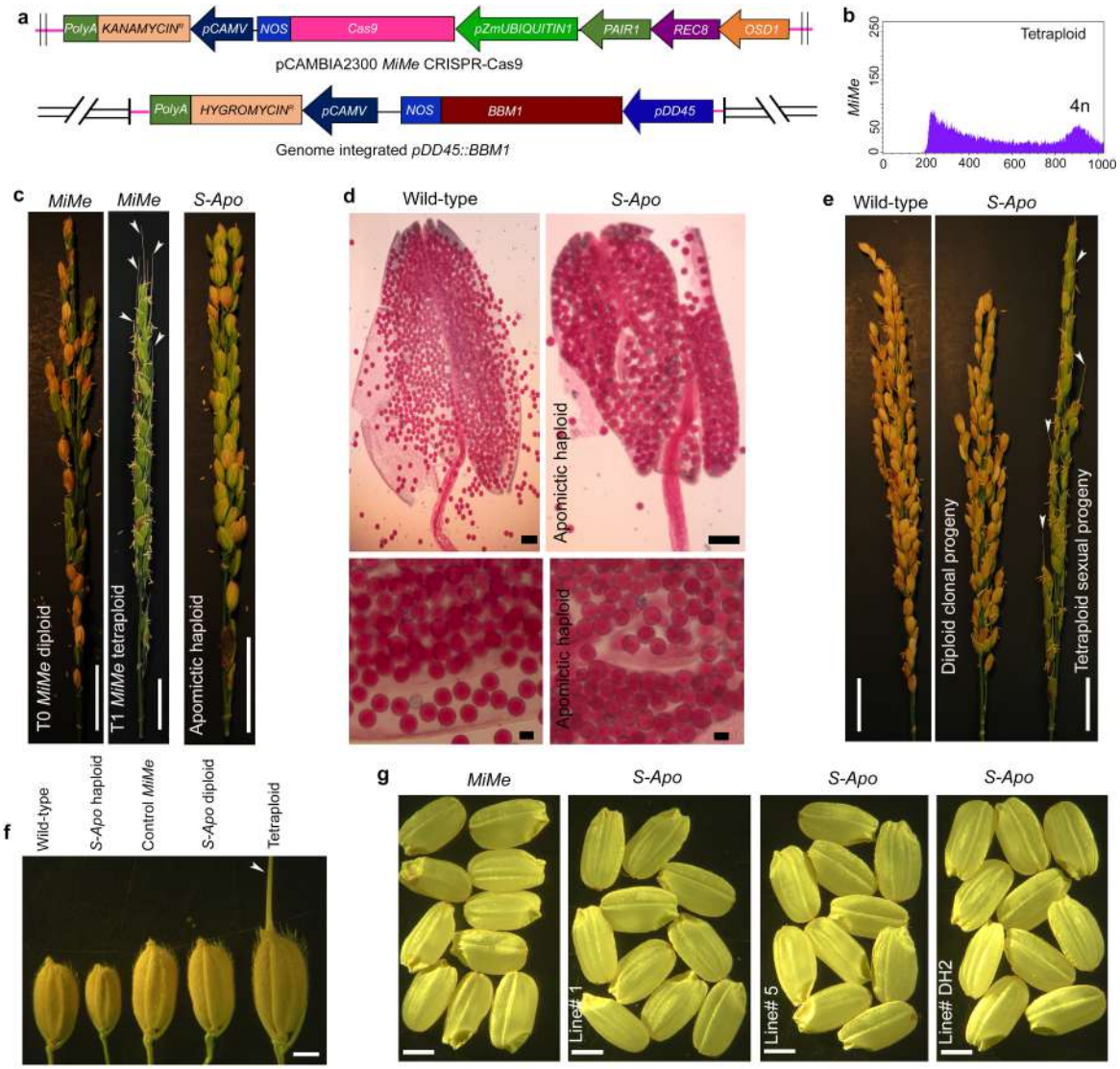

Extended Data Fig. 6 | Asexual propagation through seed in rice. **a**, Top, schematic of the CRISPR–Cas9 plasmid construct used for genome editing of the three *MiMe* rice genes. Bottom, schematic of genome-integrated *pDD45::BBM1* in the *BBM1*-ee plants. **b**, DNA histogram of flow cytometric peak showing 4*n* ploidy in T_1 progeny ($n = 33/33$ tested) of a control T_0 *MiMe* plant. **c**, Left, panicle of a control T_0 diploid *MiMe* plant with fertile seeds. Middle, a tetraploid T_1 *MiMe* panicle, exhibiting complete infertility; that is, no seed filling, and larger flowers (note scale bars), with awns (white arrowhead). Awns are normally suppressed in most *japonica* rice cultivars including Kitaake. All T_1 *MiMe* progeny ($n = 139$) were scored for the phenotype of complete infertility and presence of awns, including 33 plants that were additionally confirmed in **b** by flow cytometry. Right, panicle of an *S-Apo* haploid plant showing fertile seeds ($n = 45$). Scale bars, 2 cm. **d**, Wild-type and *S-Apo* haploid anthers, showing viable pollen ($n = 15$). Scale bars, 0.2 mm (top) and 100 μm (bottom). **e**, Comparison of panicles from wild type (left), with diploid clonal progeny (57/381) and sexual tetraploid progeny ($n = 324/381$) from a diploid *S-Apo* plant (right). The white arrowheads show awns in tetraploid. Scale bars, 2 cm. **f**, Size comparison of progeny seeds from control wild type, a synthetic *S-Apo* haploid, a control *MiMe*, a synthetic *S-Apo* diploid clone, and an infrequent (3%) filled seed produced by the sexual tetraploid progeny of an *S-Apo* diploid ($n = 100$ for each genotype). Scale bar, 2 mm. **g**, Comparison of seed size between control *MiMe*, diploid *S-Apo* line 1, diploid *S-Apo* line 5 and double-haploid *S-Apo* line DH2 ($n = 100$ for each transgenic line). No noticeable variation in seed size is observed. Scale bars, 2 mm.

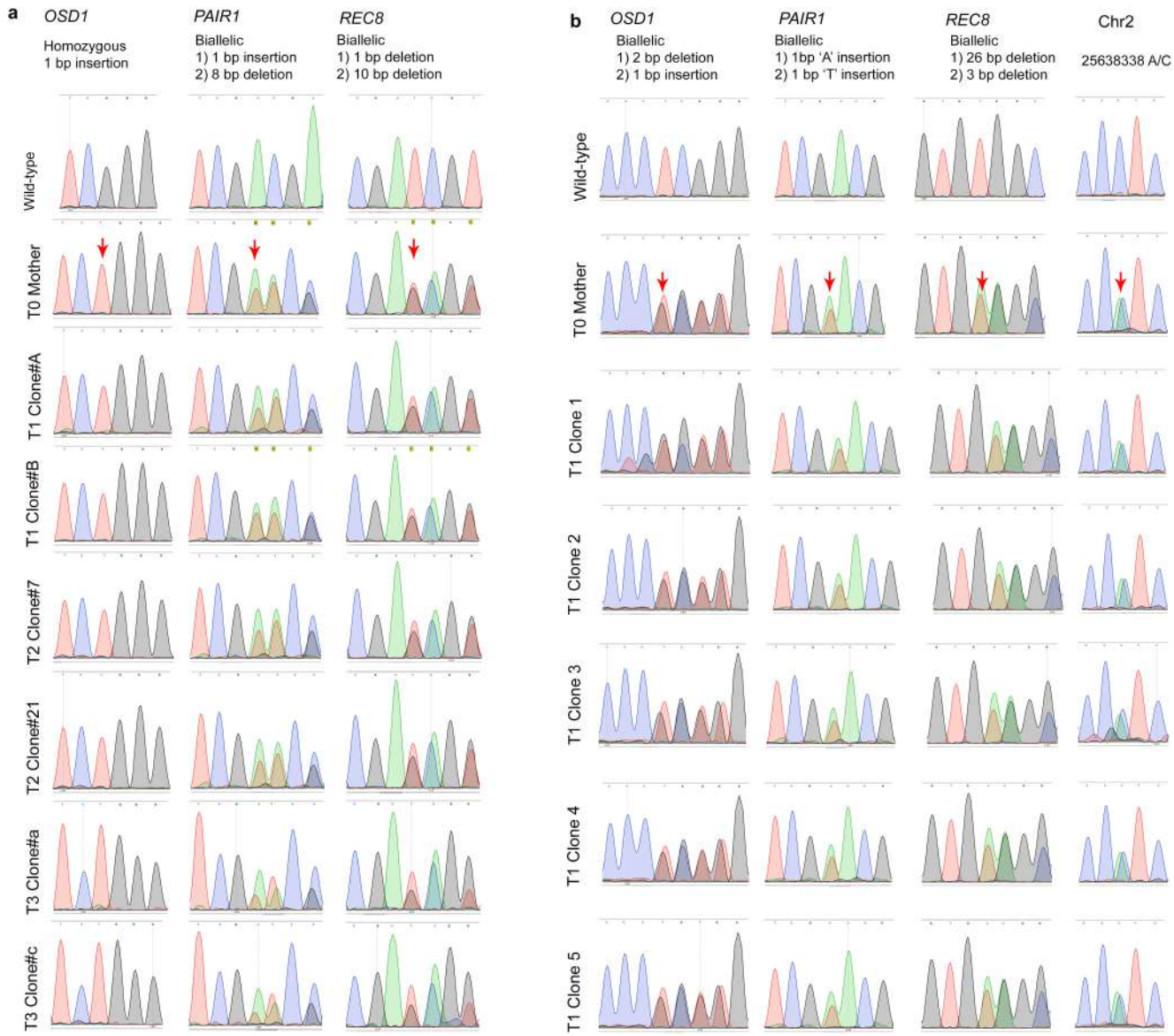

Extended Data Fig. 7 | *MiMe* mutations and confirmation of clonal progeny from *S-Apo* plants. a, Sequence chromatograms at mutation sites of *MiMe* genes in wild-type, T_0 diploid *S-Apo* mother plant and two diploid progeny from each of T_1, T_2 and T_3 generations of *S-Apo* line 1 ($n = 7$). Red arrows point to mutation sites. *PAIR1* and *REC8* are biallelic whereas *OSD1* is homozygous. **b**, Sequences of the T_0 *S-Apo* mother plant and five T_1 *S-Apo* diploid progeny at *MiMe* mutation sites and one heterozygous SNP in apomixis line 5 ($n = 6$). Red arrows show the mutation sites or SNP. All three *MiMe* mutations—*OSD1*, *PAIR1* and *REC8*—are biallelic. All progeny across different generations in both the *S-Apo* lines have same mutations as the T_0 mother plants, indicating absence of segregation and thus clonal propagation.

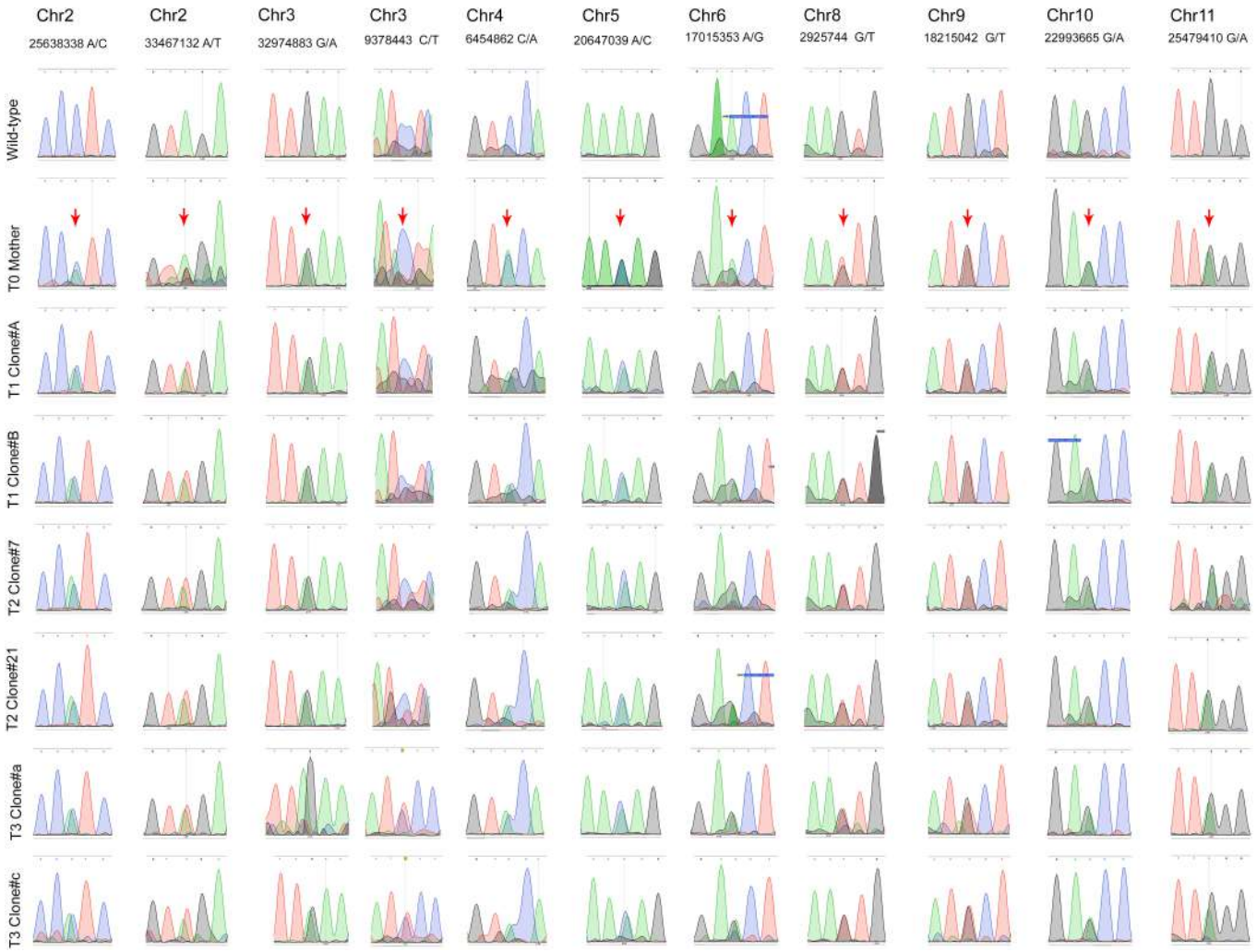

Extended Data Fig. 8 | Confirmation of SNPs by PCR. Sequence chromatograms of 11 SNPs are shown for wild-type, T_0 diploid *S-Apo* mother plant and two diploid *S-Apo* progeny from each of the T_1, T_2 and T_3 generations for line 1 ($n = 7$). All the 11 SNPs were found to be present in the T_0 mother plant and all the progeny across different generations, confirming that there is no segregation; thus clonal propagation. The red arrows show the location of the SNP. Chr, chromosome; the numbers indicate the position on the respective chromosome.

Extended Data Table 1 | Functional characterization of *BBM* genes in rice

a

Locus/Isoform	Gene	EC	SpC	Z2.5	Z5	Z9	Z2.5_JxI	Z2.5_IxJ
LOC_Os11g19060.1	*BBM1*	0	2.03	1.45	4.5	5.5	0.51	0.38
LOC_Os02g40070.1	*BBM2*	0	0	0.63	1.75	1.56	0.2	0.28
LOC_Os01g67410.1	*BBM3*	0	0.54	1.01	2.04	0.45	0.15	0.14
LOC_Os04g42570.1	*BBM4*	0	0.2	0	0	0	0.295	0

b

Number of seeds tested	Seeds germinated	Seeds that did not germinate	Percentage non-germinated	Genotypes of germinated seedlings: *BBM1/BBM1: BBM1/bbm1: bbm1/bbm1*
297	191	106	35.6	81:108:2*

c

Female *BBM1/BBM1 bbm2/bbm2 bbm3/bbm3* X Male *bbm1/BBM1 bbm2/bbm2 bbm3/bbm3*					
No. of Seeds	Seeds germinated	Wild-type for *BBM1*	Heterozygous for *BBM1*	Seeds did not germinate	Non -germinating seeds genotyped
149	121	59	62	28	23, all heterozygous**

d

Female *bbm1/BBM1 bbm2/bbm2 bbm3/bbm3* X Male *BBM1/BBM1 bbm2/bbm2 bbm3/bbm3*					
No. of Seeds	Seeds germinated	Wild-type for *BBM1*	Heterozygous for *BBM1*	Seeds did not germinate	Non-germinating seeds genotyped
67	67	35	32	0	0

a, Expression of four *BBM*-like genes in rice gametes and zygotes from previous studies[11,15] presented as reads per million averaged from three replicates. Z2.5, Z5 and Z9 columns are from isogenic *japonica* zygotes at 2.5, 5 and 9 HAP, respectively. J×I and I×J columns are hybrid zygotes from crosses, the female parent is listed first. EC, egg cell; I, *indica*; J, *japonica*; SpC, sperm cell; Z, zygote. **b**, Summary of seed viability in progeny of *BBM1/ bbm1 bbm2/bbm2 bbm3/bbm3* mutant plants. A loss of viability was observed, as around 36% (106/297) of seeds fail to germinate. Of the germinated seedlings, only 1% (2/191) were triple homozygotes, instead of the expected 25% if there is no effect of genotype on viability. **c**, **d**, Dependence of seed viability on paternal allele transmission of *BBM1*. **c**, When the *bbm1* allele is transmitted by the male parent, around 27% of the genotyped heterozygotes fail to germinate (23/(23 + 62)), despite a functional *BBM1* allele inherited from the female parent. **d**, All seeds germinate when the mutant *bbm1* allele is transmitted by the female parent ($n = 67$).
*The chi-square value for goodness-of-fit between the expected Mendelian 1:2:1 ratio and the observed data is 68.623; the corresponding right-tail P value is 1.714×10^{-15}.
**The two-tailed Fisher's exact test P value is 0.0001, for the genotyped non-germinating seeds to contain all heterozygotes and no wild types.

Extended Data Table 2 | Haploid induction and clonal propagation in rice

a

Transgenic line#	Generation	Number of plants tested	Number of haploids	% Haploid induction
1	T1	28	2	7.1
3	T1	25	2	8
4	T1	32	3	9.3
5	T1	34	2	5.8
8	T1	57	6	10.5
10	T1	27	2	7.4
11	T1	31	2	6.4
Haploid induction in homozygous T1 progeny line#8c				
8c	T2	185	54	29.2
	T3	40	13	32.5
	T4	33	9	27.2
	T5	18	5	27.7
	T6	21	6	28.5
	T7	24	7	29.1

b

Frequencies of haploid asexual progeny from haploid *S-Apo* plants					
Transgenic line#	**Generation**	**Number of plants tested**	**Number of haploids**	**Number of diploids**	**% Apomixis**
1	T1	19	5	14	26.3
	T2	31	8	23	25.8
2	T1	56	8	47	14.2
	T2	116	19	97	16.3
	T3	34	5	29	14.7
Frequencies of diploid asexual progeny from diploid *S-Apo* plants					
Transgenic line#	**Generation**	**Number of plants tested**	**Number of diploids**	**Number of tetraploids**	**% Apomixis**
1	T1	27	3	24	11.1
	T2	27	4	23	14.8
	T3	13	2	11	15.3
5	T1	41	12	29	29.2
DH#2	T2	121	14	107	11.5
	T3	123	18	105	14.6
	T4	29	4	25	13.7

a, Haploid induction in *BBM1*-ee (*pDD45::BBM1*) transgenic plants. The T_0 primary transformants were hemizygous for the *BBM1*-ee transgene. One diploid T_1 plant 8c from transformant 8 was maintained as a haploid inducer line up to the T_7 generation. **b**, Identification of synthetic haploid and diploid apomictic progeny from *S-Apo* (*MiMe* + *BBM1*-ee) plants of transformant line numbers 1 and 2 (haploids), and line numbers 1 and 5 (diploids). For T_2 and subsequent generations, propagation was performed by selecting from each generation, haploid and diploid progeny respectively. DH#2 refers to a doubled haploid derived from self-pollination of T_1 plants of the haploid apomixis line 2.

nature research

Corresponding author(s): Venkatesan Sundaresan

Reporting Summary

Nature Research wishes to improve the reproducibility of the work that we publish. This form provides structure for consistency and transparency in reporting. For further information on Nature Research policies, see Authors & Referees and the Editorial Policy Checklist.

Statistical parameters

When statistical analyses are reported, confirm that the following items are present in the relevant location (e.g. figure legend, table legend, main text, or Methods section).

n/a	Confirmed	
☐	☒	The exact sample size (*n*) for each experimental group/condition, given as a discrete number and unit of measurement
☐	☒	An indication of whether measurements were taken from distinct samples or whether the same sample was measured repeatedly
☐	☒	The statistical test(s) used AND whether they are one- or two-sided *Only common tests should be described solely by name; describe more complex techniques in the Methods section.*
☐	☒	A description of all covariates tested
☐	☒	A description of any assumptions or corrections, such as tests of normality and adjustment for multiple comparisons
☐	☒	A full description of the statistics including central tendency (e.g. means) or other basic estimates (e.g. regression coefficient) AND variation (e.g. standard deviation) or associated estimates of uncertainty (e.g. confidence intervals)
☒	☐	For null hypothesis testing, the test statistic (e.g. *F*, *t*, *r*) with confidence intervals, effect sizes, degrees of freedom and *P* value noted *Give P values as exact values whenever suitable.*
☒	☐	For Bayesian analysis, information on the choice of priors and Markov chain Monte Carlo settings
☒	☐	For hierarchical and complex designs, identification of the appropriate level for tests and full reporting of outcomes
☒	☐	Estimates of effect sizes (e.g. Cohen's *d*, Pearson's *r*), indicating how they were calculated
☐	☒	Clearly defined error bars *State explicitly what error bars represent (e.g. SD, SE, CI)*

Our web collection on statistics for biologists may be useful.

Software and code

Policy information about availability of computer code

Data collection	Microscopic images were acquired with Zeiss AxioVision 4.8.2. Flow cytometry data were obtained with Becton Dickinson CellQuest. Real time PCR data were collected with Bio-Rad CFX Manager 3.1 software from BioRad. All the sequence chromatograms were acquired with SnapGene.
Data analysis	Trimmomatic 0.38, bwa mem, GATK4.0 HaplotypeCaller, Microsoft excel, BD CellQuest, GraphPad Prism 7.

For manuscripts utilizing custom algorithms or software that are central to the research but not yet described in published literature, software must be made available to editors/reviewers upon request. We strongly encourage code deposition in a community repository (e.g. GitHub). See the Nature Research guidelines for submitting code & software for further information.

Data

Policy information about availability of data

All manuscripts must include a data availability statement. This statement should provide the following information, where applicable:

- Accession codes, unique identifiers, or web links for publicly available datasets
- A list of figures that have associated raw data
- A description of any restrictions on data availability

All the data are available from corresponding author upon suitable request .

Field-specific reporting

Please select the best fit for your research. If you are not sure, read the appropriate sections before making your selection.

☒ Life sciences ☐ Behavioural & social sciences ☐ Ecological, evolutionary & environmental sciences

For a reference copy of the document with all sections, see nature.com/authors/policies/ReportingSummary-flat.pdf

Life sciences study design

All studies must disclose on these points even when the disclosure is negative.

Sample size	Sample sizes were considered to be sufficient based on significance and effect size, no special tests were employed. In most cases, care was taken to use sample sizes that exceed the limits for normal distributions, i.e., >30. Exceptions were made only when the experimental tests were particularly labour intensive, e.g., antibody staining of sections from individual ovules. In such cases, the statistical significance test was used as the sole measure of sufficient sample size.
Data exclusions	No data were excluded.
Replication	All experimental findings were repeated or replicated at least once, in some cases by conducting a second independent analysis in parallel, e.g. the whole genome sequencing was performed on two clonal progeny from each generation. All attempts at repetition or replication were successful.
Randomization	For this type of study, randomization techniques are not applicable. However, where possible, care was taken to select plants or seeds randomly for analysis.
Blinding	Not performed, because of inapplicability to this study

Reporting for specific materials, systems and methods

Materials & experimental systems

n/a	Involved in the study
☐	☒ Unique biological materials
☐	☒ Antibodies
☒	☐ Eukaryotic cell lines
☒	☐ Palaeontology
☒	☐ Animals and other organisms
☒	☐ Human research participants

Methods

n/a	Involved in the study
☒	☐ ChIP-seq
☐	☒ Flow cytometry
☒	☐ MRI-based neuroimaging

Unique biological materials

Policy information about availability of materials

Obtaining unique materials	All unique materials used are readily available from the authors.

Antibodies

Antibodies used	Rabbit anti-GFP antibody (ab6556, Abcam, Cambridge, UK) was used as primary antibody for immunohistochemistry and goat anti-rabbit AP conjugate (A9919, Sigma-Aldrich, USA) as secondary antibody.
Validation	Validation: Primary rabbit anti-GFP antibody (Abcam, ab6556) was used at a dilution of 1:1000. Secondary goat anti-rabbit AP conjugate (Sigma-Aldrich, A9919) antibody was used at a dilution of 1:200. Anti-GFP antibody has been used for immunohistochemistry previously and shown to react with GFP epitopes in several plant species (Li et al., Nature Communications. 2018; Figueroa-Yañez et al., PLoS One, 2016), Drosophila (Hamp et al., Journal of Cell Science, 2016), mice (Tang et al., The Journal of Neuroscience, 2015) etc (for details https://www.abcam.com/gfp-antibody-ab6556.html). Goat anti-rabbit secondary antibody has been tested previously in plants (Reichelt, et al., The Plant Journal, 1999), Xenopus (Almeida et al., Neural Development 2010) and other species (https://www.sigmaaldrich.com/catalog/product/sigma/a9919?lang=en&region=US).

Flow Cytometry

Plots

Confirm that:

☐ The axis labels state the marker and fluorochrome used (e.g. CD4-FITC).

☒ The axis scales are clearly visible. Include numbers along axes only for bottom left plot of group (a 'group' is an analysis of identical markers).

☐ All plots are contour plots with outliers or pseudocolor plots.

☒ A numerical value for number of cells or percentage (with statistics) is provided.

Methodology

Sample preparation	Leaf tissue were chopped with a razor blade.
Instrument	Becton Dickinson FACScan system
Software	Becton Dickinson CellQuest
Cell population abundance	All the leaf cells used for flow cytometry are same.
Gating strategy	Only the initial debris was gated out.

☐ Tick this box to confirm that a figure exemplifying the gating strategy is provided in the Supplementary Information.